Assessment of Spring-run Chinook Salmon Spawning during 2019 within the San Joaquin River, California

Annual Technical Report

SAN JOAQUIN RIVER
RESTORATION PROGRAM

[This page intentionally left blank.]

Assessment of Spring-run Chinook Salmon Spawning during 2019 within the San Joaquin River, California

Prepared by:

Austin Demarest[1], Andreas Raisch[1], Lauren Yamane[1], Lori Smith[1*], and Andy Shriver[2]

[1] U.S. Fish and Wildlife Service, 850 S. Guild Ave, Suite 105, Lodi California 95240
[2] California Department of Fish and Wildlife, 1234 E. Shaw Avenue, Fresno, California 9371
To whom correspondence should be addressed: lori_smith@fws.gov

The preferred citation for this report is:

Demarest, A., A. Raisch, L. Yamane, L. Smith, and A. Shriver. 2021. Assessment of Spring-run Chinook Salmon Spawning during 2019 within the San Joaquin River, California. San Joaquin River Restoration Program Annual Technical Report. U.S. Fish and Wildlife Service, Lodi, California.

July 2021

[This page intentionally left blank.]

Table of Contents

Abbreviations and Acronyms

AICc	Akaike Information Criterion with Correction for Finite Sample Sizes
ATU	Accumulated Thermal Unit
C	Celsius
CDEC	California Data Exchange Center
CDFW	California Department of Fish and Wildlife
cfs	Cubic Feet per Second
CWT	Coded Wire Tag
DO	Dissolved Oxygen
DWR	California Department of Water Resources
ETF	Egg-to-Fry
FDX	Full-Duplex
FL	Fork Length
FRFH	Feather River Fish Hatchery
FWQ	Friant Water Quality California Data Exchange Center Gage
GLM	Generalized Linear Model
GPS	Global Positioning System
H41	Highway 41 Bridge California Data Exchange Center Gage
HDX	Half-Duplex
kHz	Kilohertz
m	Meter
m^2	Meter Squared
m/s	Meter per Second
mg/L	Milligram per Liter
mm	Millimeter
n	Sample Size
NMFS	National Marine Fisheries Service
NTU	Nephelometric Turbidity Unit
PIT	Passive Integrated Transponder
rkm	River Kilometer
Reclamation	U.S. Bureau of Reclamation
SCARF	Salmon Conservation and Research Facility
Settlement	Stipulation of Settlement in Natural Resources Defense Council [NRDC], et al. vs. Kirk Rodgers, et al. 2006
SD	Standard Deviation
SJF	San Joaquin River below Friant California Data Exchange Center Gage
SJRRA	San Joaquin River Restoration Area
SJRRP	San Joaquin River Restoration Program
SRCS	Spring-run Chinook Salmon
U.S.	United States
USFWS	U.S. Fish and Wildlife Service

List of Tables

List of Figures

Executive Summary

Construction of Friant Dam was completed in the 1940's resulting in the exclusion of the majority of historic Chinook Salmon (*Oncorhynchus tshawytscha*) spawning habitat. Increased water diversions following impoundment led to the extirpation of fall-run and spring-run Chinook Salmon (SRCS) from the San Joaquin River upstream of the confluence with the Merced River to Friant Dam, hereinafter referred to as San Joaquin River Restoration Area (SJRRA). The San Joaquin River Restoration Program (SJRRP) is a multiagency collaborative program that is focused on restoring the river to develop and maintain naturally reproducing and self-sustaining populations of Chinook Salmon. Since the initiation in 2009, the SJRRP has prioritized maintaining river connectivity with dedicated restoration flows, restoring volitional passage, and establishing a broodstock population of SRCS. Currently, the quantity and quality of suitable spawning habitat available within the SJRRA is unclear. To address this uncertainty, we report on spawning activity and egg-to-fry (ETF) survival from SRCS. From 2014 to 2018, juvenile SRCS were released annually below fish passage barriers of the SJRRA to initiate reintroduction. Adult SRCS could have returned to the SJRRA as early as 2016, as a result of the previous juvenile releases. However, in 2019, the SJRRP captured and successfully released naturally returning hatchery adult SRCS. During redd monitoring and carcass surveys in 2019, we documented an unprecedented number of unmarked salmon spawning within Reach 1, suggesting that SRCS volitionally returned, bypassing all fish passage barriers, taking alternate routes available with flood flows in the spring of 2019. This was later confirmed with a greater number of redds than adult female SRCS released in Reach 1 of the SJRRA. Throughout the redd monitoring and carcass survey, SRCS carcasses (volitional hatchery return) were recovered. Although we confirmed 149 volitional hatchery returns with carcasses, we were unable to quantify the total number of SRCS entering the SJRRA. Redd size and physical characteristics were consistent with natural SRCS redds reported in other studies, as were pre-redd substrate composition assessments. We observed higher temperatures (>17°C) in 2019, while also documenting a more restricted spatial distribution of spawning than 2018. Spawning activity in 2019 occurred between September 10 and November 11. In addition to the recovery of volitional return hatchery carcasses, we recovered nine female and seven male broodstock along with two female and one male translocated carcasses. From the carcasses recovered, 89 percent of broodstock, 50 percent of translocated hatchery returns, and 92 percent of volitional hatchery returns fully spawned. We observed a mean of 702 fry emerge from 12 redds monitored with emergence traps, much higher than the mean of 28 fry that emerged from 10 trapped redds in 2018. During incubation and emergence, redds in 2019 were exposed to lower water temperatures and flows and higher dissolved oxygen. Redds in 2019 were also found in areas with a higher pre-redd sand composition than 2018, suggesting quality spawning habitat may be limited. Based on these results from a small sample size, we recommend that the SJRRP continue SRCS redd, adult carcass, and fry emergence surveys. Additional efforts to distinguish redds created by broodstock and volitional hatchery returns will enable potential differences in ETF survival between groups. It is recommended that emergence studies be expanded to identify whether emergence traps affect ETF survival (i.e., trap effects studies are beginning in 2020). These additional studies will provide invaluable information to determine restoration requirements for the successful reestablishment of SRCS within the San Joaquin River.

Introduction

Historically, the main-stem San Joaquin River and upper watershed tributaries annually produced up to approximately 500,000 spring-run, fall-run, and late fall-run Chinook Salmon (*Oncorhynchus tshawytscha*) and supported the southernmost spring-run populations in North America (Fry 1961; Fisher 1994; Yoshiyama et al. 2000). Salmon runs are distinguished by the time of year adults return to fresh water, the elevation and type of reaches used for spawning activity, the duration of juvenile residence period, and the time of juvenile emigration. Adult spring-run Chinook Salmon (SRCS) traditionally returned in the spring and used cold pools in higher elevations for summer holding followed by late summer/early fall spawning in upper tributary streams (Yoshiyama et al. 1998). Adult fall-run and late fall-run Chinook Salmon return in the fall and use lower elevation habitats near the valley floor for late fall/early winter spawning (Fisher 1994; Meyers 2019). After construction of Friant Dam, habitat for Chinook Salmon and other native fish have become degraded, dewatered, and fragmented due to increased groundwater pumping and water diversions (Fry 1961; Warner 1991; Yoshiyama et al. 2001). Along the San Joaquin River, mining for aggregate within the channel and floodplains left large deep pits that provide suitable habitat conditions for black basses (*Micropterus* spp.) and other predators of juvenile salmon (Williams 2006). The cumulative effects of these actions resulted in the rapid decline of Chinook Salmon runs within the San Joaquin River above the confluence of the Merced River and the extirpation of SRCS by 1950 and remaining runs shortly thereafter (Fry 1961; Fisher 1994; Yoshiyama et al. 2001; Williams 2006). Chinook Salmon still occur in the major tributaries of the lower San Joaquin River such as the Merced, Stanislaus, and Tuolumne Rivers (Yoshiyama et al. 2000).

In 2006, a Settlement (Natural Resources Defense Council [NRDC], et al. vs. Kirk Rodgers, 2006) was reached between NRDC, Friant Water Users Authority, and the U.S. Departments of the Interior and Commerce to help develop and enact Restoration and Water Management Goals on the San Joaquin River below Friant Dam to the confluence of the Merced River (SJRRP 2010). The Restoration Goal established by the Settlement focuses on restoring and maintaining natural fish populations in "good condition" in the San Joaquin River Restoration Area (SJRRA) including naturally reproducing salmon and other native fish species. Interim flow to support SJRRP began in 2009 and concluded in 2014, in conjunction with Restoration Flows.

However, it wasn't until 2016 that the river was fully connected. Additionally, the Settlement's Water Management Goal is to reduce and/or avoid the impact of adverse water supply on the Friant Division long-term contractors that may result from these Interim and Restoration Flows in the SJRRA. Consequentially, the San Joaquin River Restoration Program (SJRRP) was formed to develop comprehensive plans and actions to achieve these goals. The SJRRP is a multiagency collaborative program between the U.S. Fish and Wildlife Service (USFWS), the U.S. Bureau of Reclamation (Reclamation), National Marine Fisheries Service (NMFS), the California Department of Fish and Wildlife (CDFW), and the California Department of Water Resources (DWR).

Current SJRRP efforts are focused on managing river temperature, restoring volitional passage, and restoring SRCS to the SJRRA through the development of an experimental population of Chinook Salmon using broodstock from the Feather River Fish Hatchery (SJRRP 2018b). Ongoing habitat restoration efforts will support the anticipated future growth in the salmon population. The SJRRP's reintroduction strategy includes annual releases of juvenile SRCS below fish passage barriers and annual releases of sexually mature excess adult broodstock SRCS from the Salmon Conservation and Research Facility (SCARF) into Reach 1 spawning grounds, the most upstream area of the SJRRA (SJRRP 2011, Figure 1).

The Fisheries Management Plan (FMP) of the SJRRP has established several criteria to guide restoration activities to achieve salmon population viability within the SJRRA (SJRRP 2010). A major component of data collection has focused on SRCS spawning success (i.e., production of offspring from spawning adults) of individuals within the population and understanding the causes of associated variability. One objective of the FMP suggests that an in-river egg-to-fry (ETF) survival rate of ≥ 50 percent for SRCS is needed to achieve the SJRRP's population target. The FMP also identifies the need to monitor for superimposition among redds because it may reduce ETF survival and limit the ability for the SJRRP to reach production goals. Superimposition occurs when a female salmon selects nearly the same location to build a redd as that occupied by a preexisting redd and then scours and/or deposits substrate on the preexisting redd. Previous studies have shown that superimposition increases as the density of female spawners increases and has been attributed to limited spawning habitat (McNeil 1964; Weeber et al. 2010). The FMP also includes a population objective to achieve an annual minimum of 500 naturally produced adult SRCS spawning successfully. Annual redd, carcass, and emergence survey efforts described in this report will allow the SJRRP to identify inadequacies in suitable spawning habitat and assess population viability within the SJRRA.

Reintroduction efforts began in 2014 with juvenile hatchery releases and, after spending a minimum of two years through adulthood in the ocean, were expected to return as early as 2016 to the river to spawn. However, returning adults were not observed until 2019. From 2016 to 2019, 161 female and 272 male excess adult broodstock from the SCARF were released directly into Reach 1 of the SJRRA. Adult SRCS were released by the SJRRP as a proxy for natural returns with the assumption that broodstock have similar spawning habitat preferences and success. The objective of the adult releases are to assess the holding and spawning habitat quality and quantity within Reach 1.

In spring 2019, 23 naturally returning adults were captured in Reach 5 of the SJRRA during SRCS adult trap and haul operations. Twenty were successfully transported and released into Reach 1. Later, one of the released natural returns was recovered as a pre-spawn mortality within the Highway 99 rotary screw trap. Additionally, higher than average seasonal precipitation during the 2019 return migration season resulted in Flood Flow releases from Friant Dam, allowing volitional passage of SRCS past in-river barriers into Reach 1 (NRCS 2019). This was the first observation of SRCS naturally returning, bypassing passage barriers. The presence of hatchery-released broodstock, translocated or trap and haul, and volitionally returned adults allowed the observation of spawning habitat preference, behavior, and success as well as comparisons between the three groups. In this document, we present results from redd, carcass, and emergence trapping studies of SRCS in 2019 within Reach 1 of the SJRRA and compare the results to those from prior years.

Redd Monitoring and Carcass Survey Objectives

Routinely, redd monitoring has been used to assess Pacific salmonid *Oncorhynchus spp.* escapement, abundance, spawn timing, and collect physical measurements of salmon nests (Gallagher et al. 2007). Redd monitoring and carcass surveys for SRCS in the SJRRA began in 2016 and have continued annually. The purpose of redd monitoring within the SJRRA is to provide the SJRRP with information about reproductive behavior, spawn timing, habitat use, and availability for SRCS. Carcass surveys are conducted simultaneously to assess length, conditions, spawn status, and collect biological samples for additional studies. Redd monitoring and carcass surveys were conducted in Reach 1 for the SJRRRA in 2019 to document the following for reintroduction:

1) Quantify SRCS spawning activity within Reach 1 of the SJRRA.
2) Document the spatial and temporal distributions of SRCS spawning activity and the associated habitat characteristics of spawning site selection.
3) Document the prevalence of redds that exhibit superimposition.
4) Assess and compare the physical and environmental characteristics of redds created in 2019 with 2018 and prior years where data are sufficient.
5) Describe the spatial trends of carcasses recovered within the SJRRA.
6) Determine proportions of age classes recovered as carcasses within the SJRRA.

Emergence Trap Survey Objectives

In the past, emergence traps have been used as a method to assess ETF survival and associated environmental characteristics that may affect emergence from the hyporheic environment for Chinook Salmon in the San Joaquin and Tuolumne Rivers (TID/MID 1991; Meyers 2019). The SJRRP initiated emergence trapping of SRCS redds in 2018 and this effort is ongoing. The goal of the implementation of this survey is to enumerate the number of SRCS eggs that successfully developed and emerged as fry from redds in the SJRRA. Associated physical and chemical water quality characteristics including substrate composition, velocity, temperature, dissolved oxygen (DO), and turbidity were collected to gain a better understanding of characteristics that may influence ETF survival. The emergence trap survey was used to accomplish the following objectives:

1) Determine the number of fry that successfully emerge from trapped redds and develop ETF survival estimates for 2019 to compare with ETF survival from 2018.
2) Determine environmental variables affecting ETF survival rates.
3) Document emergence timing for SRCS.

Methods

Study Area

The SJRRA is approximately 240 river kilometers (rkm) long and separated into five reaches beginning at Friant Dam and ending at the confluence of the Merced River (Figure 1). The SJRRA is located within the San Joaquin Valley and is characterized by a Mediterranean climate with wet-cool winters and dry-hot summers (Null and Viers 2013). Historically, the San Joaquin River flowed from the high elevations of the Southern Sierra Nevada Mountain Range, meandered southwest until it reached the Central Valley, continued northwest to the Sacramento-San Joaquin Delta, and emptied into the Pacific Ocean (Galloway and Riley 1999). The San Joaquin Basin is dependent upon annual snowpack and the subsequent meltwater that replenish Millerton Lake above Friant Dam.

Since the Settlement, the SJRRA has been reliant upon dedicated Restoration Flows from the water stored within Millerton Lake. However, extensive agricultural land use within the San Joaquin Valley has subjected the San Joaquin River Basin to water diversions, as well as large-scale groundwater and riparian pumping operations to support agriculture (Galloway and Riley 1999; Null and Viers 2013; Traum et al. 2014). As a result, downstream reaches of the SJRRA have high effluent discharge from agriculture runoff and flow targets are determined by the Water Year type, the Restoration Administrator's flow recommendations, and compliance requirements for holding contracts to maintain minimum flows at the downstream end (i.e., at Gravelly Ford) of Reach 1 (SJRRP 2017, Figure 1).

In Reach 1, flows are conveyed through a moderately sloped incised gravel-bedded channel that is confined by periodic bluffs or terraces. The reach contains off-channel and in-channel mine pits from historic sand and gravel mining operations (SJRRP 2010). Currently, land use within Reach 1 to Reach 5 of the SJRRA is dominated by anthropogenic urban and agricultural developments (Traum et al. 2014). However, the prioritization of agricultural practices and long-term operations of dams, water bypasses, diversions, and groundwater pumping caused the natural river to run dry in most years, subsequently degrading habitat for native fish.

Currently, a connected river is available via the Eastside Bypass, restricting volitional passage of SRCS to wetter years when spring floods flow through the Chowchilla Bifurcation Structure. Based on historical spawning surveys and modeled in-river temperatures, suitable spawning habitat for Chinook Salmon is thought to be restricted to the first 8 to 11 rkm below Friant Dam within Reach 1 of the SJRRA during drier water years (Gordon and Greimann 2015). However, the quantity and quality of suitable SRCS habitat within Reach 1 needs further assessment for achieving the SJRRP's spawning habitat objectives during the Reintroduction Phases. To address these needs, SRCS redd, carcass, and emergence surveys were conducted by the SJRRP on the San Joaquin River in Reach 1 of the SJRRA from below Friant Dam (rkm 431) to the Milburn Ecological Unit (rkm 398; Figures 2 and 3).

Study Specimens

In 2019, the SJRRP had a unique opportunity to study translocated, volitional returning, and excess broodstock adult SRCS in Reach 1. For visible distinction, fish were tagged sub-dermally with different colored and uniquely numbered Floy T-bar anchor fish tags (Floy Tag and Mfg., Inc, Seattle, Washington) on the dorsal fin insertion. Translocated fish were marked with orange T-bar tags. May broodstock release males were marked with purple tags and females with green tags. August broodstock release males were marked with red tags and females with blue tags. Tag colors helped with distinguishing sex and the release group during spawner surveys.

In addition to the external tags, Vemco (Innovasea Inc., Bedford, Nova Scotia, Canada) V9 69 kHz acoustic tags and Oregon RFID 23 mm half-duplex (HDX) passive integrated transponder (PIT) tags were implanted intra-gastrically with a balling gun. All translocated adults and all female broodstock were implanted with both acoustic and PIT tags. However, due to tag availability, only 14 broodstock males were implanted with acoustic tags. Acoustic tags were injected with the intent to track behavior and habitat selection through spawning. In concert with acoustic tags, HDX tags were injected with the intent to link individual fish to their successive redd as part of a separate effort by CDFW (Shriver 2015a; Shriver 2017). All broodstock were also tagged with full-duplex (FDX) PIT tags to identify individuals while being reared at SCARF until they were released into the SJRRA. The FDX tags helped identify fish when all the other tags were lost. Translocated fish consisted of 13 female, 6 male, and 1 unknown gender SRCS that were captured in Reach 5 and trucked upstream for release into Reach 1. The first and third of the translocated adults were released at Owl Hollow (rkm 416). The remaining 18 were released at Camp Pashayan, immediately upstream of California State Route 99 (rkm 389). Broodstock releases occurred twice in 2019: first in May at Owl Hollow (rkm 416) consisting of 7 females and 39 males, and second in August at Ball Ranch (rkm 422) consisting of 48 males and 30 females (CDFW 2019; Figure 4).

Redd Monitoring and Carcass Surveys

Redd monitoring and carcass surveys were conducted between August 27 and November 11, 2019. Surveys were restricted to daylight hours and ideal weather conditions (e.g., without heavy rain). The survey area was divided into three sections to ensure complete spatial coverage from Friant Dam (rkm 431) to Lost Lake (rkm 426), Lost Lake to the Fresno County Sportsmen's Club (rkm 413), and the Fresno County Sportsmen's Club to the Milburn Ecological Unit (rkm 398; Figures 2 and 3). Surveys occurred two to four times per week during the study period, depending on the extent of spawning activity.

Surveys were conducted from a drift boat and kayaks like previous years. The drift boat was a tool used to help survey the thalweg and deep pools; likewise, kayaks were used to help staff survey channel margins and other areas inaccessible to the drift boat. Kayakers paddled ahead and surveyed riffles before guiding the drift boat downstream to minimize disturbance of new and/or ongoing spawning activity. Kayakers traversed upstream of each riffle for an initial inspection of spawning activity prior to proceeding to the shoreline to walk down the riffle with their kayak for a more thorough visual inspection of spawning activity, areas freshly cleared of periphyton, redds, and carcasses. Areas cleared of periphyton were further investigated to determine if it was caused by potential spawning activity or water hydraulics. These areas were documented and observed during successive weeks to see if a pit and defined tailspill developed. Redds and carcasses discovered were processed according to the methods listed below.

Typically, surveys are completed with one drift boat and two kayaks and this effort occurred during the first three survey weeks. However, after the discovery of SRCS carcasses without tags and observations of untagged fish within spawning habitat, spawner survey effort was increased by one additional day. To ensure optimal spatial coverage during weeks four to six, when more spawning activity was observed, three additional staff members and two kayaks were added to the survey. Surveys were also adjusted spatially, and by the quantity of spawning activity. This included surveying the two upstream survey sections twice weekly and excluding the third most downstream survey section, which lacked spawning.

Mobile Acoustic Monitoring Survey

Fish location data were collected from a drift boat via Vemco VR-100 mobile acoustic receiver in conjunction with a 50 to 80 kHz omni-directional hydrophone to detect SRCS with acoustic tags. While surveying, the hydrophone was positioned so that it was submersed below the water surface while the drift boat proceeded downstream. Following an acoustic detection, the tag identification number, GPS location, signal detection strength and time was recorded. Concurrently, water temperature was also recorded. These detections were relayed to kayakers to help them be cognizant of fish in upcoming riffles and to proceed with caution to minimize disturbance. If a kayaker visually observed a SRCS on a redd, the drift boat pulled over to the adjacent shoreline, detached the omni-directional hydrophone, attached the directional hydrophone, and identified which acoustic tagged SRCS was likely associated with that redd. If multiple fish were detected in an area and the identification of individual fish occupying each redd could not be distinguished, kayakers then recorded colors of T-bar tags to help link individuals to each redd. The use of the directional hydrophone and observation of T-bar tags was done at a distance to minimize disturbance to spawning activity behavior.

Redd Identification and Measurements

Redds were identified based on freshly exposed substrate cleared of periphyton, a substrate depression into the streambed (pit), and a mound of coarse substrate (tailspill). Redds were given a redd identification number and labeled sequentially to help denote the order of discovery and to estimate emergence timing. Substrate areas that were cleared of periphyton but lacking a tailspill were classified as a test redd and given a test redd identification number. Test redds were monitored during subsequent survey weeks for potential development into a completed redd. If a test redd developed further and had both a pit and a tailspill, it was then given the next sequential redd identification number. After redds were assigned an identification number, GPS location was recorded, a cattle ear tag fastened to a weight was placed adjacent to the pit towards river center, and flagging with the redd identification number was attached to riparian vegetation on the nearest shoreline perpendicular to flow. These markers were used to help locate surveyed redds each week to monitor how they changed throughout the survey period, identify superimposition, and locate suitable redds for emergence trap installation. Locations were recorded with an EOS Arrow-100 GNS sub-meter GPS paired with an iPhone 7 and plotted in real time in ArcGIS Online. Velocity and depth measurements were taken with an OTT MF Pro Flow meter and top set rod. Pre-redd depth and velocity measurements were taken at undisturbed substrate upstream of the redd pit. Pit depth measurements were taken at the deepest part of the pit (pit depth) and the tailspill minimum depth was taken at the shallowest point of the tailspill (tailspill crest). Length and width measurements were taken to the nearest 0.01 meter (m) for the pit and tailspill as well as a length measurement for start of the tailspill to the crest (Figure 5).

Habitat characteristics for each redd was also recorded and included channel type, channel position, and habitat type. Channel type was categorized as either main channel or side channel where the main channel was defined as the cross-section of the wetted river channel that contained the majority of the flow (i.e., greater than 50 percent of the flow) and side channel contained the minority (i.e., less than 50 percent of flow). Channel position while facing downstream was used to document where each redd was within the river (river right, river left, or river center). Habitat type was categorized based upon depth, velocity, and water surface turbulence and consisted of five categories (glide, riffle, run, pool, and backwater). Glides were shallow slow flowing (< 0.5 m depth, < 0.3 meters per second [m/s]) stretches with little or no surface turbulence, riffles were shallow fast (< 0.5 m depth, ≥ 0.3 m/s) reaches, with turbulent water and some partially exposed substrate, runs were deep and fast (≥ 0.5 m depth, ≥ 0.3 m/s) flowing reaches with little surface agitation and no major flow obstructions, pools were deep (≥ 1 m depth), low-velocity areas of water (< 0.3 m/s) with a smooth surface, and backwaters were distinct out-pockets along river margins that were relatively shallow (< 0.5 m depth) and possessed slow moving, or stagnant water (< 0.3 m/s).

Redds were assigned an age to monitor degradation and superimposition. The remaining redds were aged weekly on a 1 to 5 scale. An age 1 redd had clean rocks with no defined pit or tailspill. This was considered a test area or a redd under construction. Age 2 redds were clearly visible with clean substrate and a well-defined pit and tail spill. Age 3 redds had aged substrate, flattened tail spill, fine sediment deposition in the pit, and/or algal growth. Age 4 were old and difficult to discern, and Age 5 redds had no visible traces of a redd, only the marker denoted the location of a previously identified redd. Superimposed redds that had new substrate material in the redd area were documented as being impacted by deposition, whereas preexisting redd areas that had features excavated by a new spawning event were considered to have been scoured. If a preexisting redd experienced both, scour and deposition was recorded. After an observation of superimposition, redds were no longer aged for degradation because superimposition inhibited the accuracy of correct aging, and in some cases tailspill location.

To document the streambed substrate in spawning areas selected by salmon, substrate composition and relative substrate size were visually assessed in a 1-m^2 area directly upstream of incision of the pit of each redd (pre-redd area). Textural facies in pre-redd areas were classified according to methods established by Buffington and Montgomery (1999). The percent of fine sediment (sand, ≤ 2.0 mm) in the pre-redd area was recorded. However, if the composition of sand was < 5 percent, then percent of fine sediment was simply recorded as < 5 percent. Classification was made according to the proportional composition of the grain sizes (i.e., sand [< 2.0 mm], gravel [2.0 to 63 mm], and/or cobble [> 63 mm]) in ascending order from least abundant to most abundant. For example, if an area had 15 percent sand, 30 percent cobble, and 55 percent gravel it would be recorded as SCG, where S is sand, C is cobble, and G is gravel. Grain size was confirmed with a gravelometer by measuring the b-axis, where the a-axis is the longest length measurement of each grain and the b-axis is the second largest length (i.e., intermediate axis). If a grain size comprised ≤ 5 percent, it was omitted from the textural facies classification (i.e., CG). If the most dominant grain size was ≥ 90 percent, only this dominant grain size was included (i.e., G).

Carcass Processing

Origin (e.g., volitional hatchery return) of carcasses encountered during surveys were categorized based on the presence of T-bar tags, PIT tags, and acoustic tags. Carcasses discovered with tags were identified as either broodstock or translocated. If tags were absent, they were designated as volitional return carcasses and later confirmed as a volitional hatchery return with extracted coded wire tags (CWTs). Coordinates for each carcass, channel type, channel position, and habitat type were recorded.

Carcasses were classified by level of decomposition (fresh, decayed firm, decayed soft, or skeleton). Decomposition was designated by eye clarity, blood remaining in the gills, and the state of tissue decay. Carcasses with clear eyes and blood remaining in the gills were classified as "fresh", while fish with cloudy eyes and no blood in the gills were considered to be "decayed firm" or "decayed soft". Muscular tissue of carcasses categorized as "decayed firm" had stiff tissue, whereas carcasses categorized as "decayed soft" had a less firm muscular tissue, but were mostly intact. Fish carcasses that were more decayed, had a substantial quantity of missing muscular tissue, and were falling apart were classified as a skeleton.

Sex for each carcass was established by dissection with the presence of testes or ovaries/eggs in the peritoneal cavity. Spawn status for female carcasses was determined by the approximate quantity of eggs remaining (≤ 1,200 for spawned, 1,201 to 2,800 for partially spawned, or ≥ 2,801 for unspawned). Spawn status categories were established based on <30, 30 to 70, and > 70 percent of 4,000 eggs. The average fecundity from SCARF broodstock and Feather River Fish Hatchery (FRFH) natural returns from 2016 to 2019 was 3,879 eggs per female; therefore, 4,000 eggs were used as a fecundity baseline for estimating spawn status (P. Adelizi, CDFW, personal communication, 2020). If a carcass was too decayed, sex was recorded as unknown. Sex, spawn status, and fork length measured to the nearest millimeter were documented. The presence or absence of an adipose fin was recorded, with lack of an adipose fin indicating hatchery origin. All carcasses were photo documented with the fish lying on its right side with a measuring tape and identification tag (refer to Figure 6).

Heart tissue samples of all translocated and volitional returning SRCS carcasses were collected for parentage analysis in 2019. Heart tissue samples approximately 1 cm^2 were collected by dissection of the pericardial cavity. Samples were stored in 2 ml screw cap vials filled with 70 percent ethanol. Heads and tags of all carcasses were collected and preserved. After the survey season, CWTs, otoliths, and eyes were extracted and preserved from heads. CWTs were read with a Magniviewer Coded Wire Tag Microscope to identify origin, brood year, release date, and release location, in addition to the total number of fish per release group. Otoliths and eyes were extracted for isotope analysis to identify juvenile salmon rearing habitat in the SJRRA.

Emergence Trap Surveys

The 2019 emergence trap installation and monitoring study was conducted October 31, 2019 to February 13, 2020. Emergence traps were placed on certain redds to allow for a distribution across riffle complexes in Reach 1 and over redd creation dates. Due to limitations in the emergence trap design, the redds selected had to be accessible on foot, of appropriate size, and at moderate depths and water velocities. Twelve redds were chosen based on these constraints (Figure 2). The trap installation, monitoring, and removal schedule was based on the calculation of accumulated thermal units (ATUs), or cumulative temperature over time, where 1 ATU = 1°C for 1 day (Beacham and Murray 1990; Berejikian et al. 2011). For each emergence trapped redd, we calculated ATUs by adding average daily water temperatures over the incubation and emergence period (i.e., from date of redd discovery to trap removal) from the closest California Data Exchange Center (CDEC) station gage(s), which included Friant Water Quality (FWQ; rkm 430), San Joaquin below Friant (SJF; rkm 428), and/or Highway 41 Bridge (H41; rkm 410). Redds at or upstream of rkm 429 were assigned FWQ, redds downstream of rkm 429 and upstream of rkm 423 were assigned SJF, and those downstream of rkm 423 and upstream of rkm 414 were assigned SJF/H41 for temperatures. Each redd was covered with an emergence trap once it reached 600 ATUs, approximately five days prior to the onset of emergence. Prior fall-run Chinook Salmon surveys in Reach 1 suggested that emergence would start around 650 ATUs with peak emergence occurring between 750 and 1,000 ATUs and emergence ending by 1,700 ATUs (Castle et al. 2016a; Castle et al. 2016b; TID/MID 1991). Thus, emergence traps were intended to be removed after reaching 1,700 ATUs. Early installation and removal after 1,700 ATUs ensured that all fry were captured during emergence.

The emergence trap design was modeled after the Lower Tuolumne Don Pedro Project Fisheries Study report (TID/MID 1991) that consisted of two metal frames fastened together with hose clamps. The frames were tear drop-shaped, measuring approximately 2.42-m long by 1.83-m wide at the widest point, then decreasing in width towards the tail end with an approximate area of 2.83 m^2. A net consisting of 0.32 cm nylon mesh surrounded by a blue canvas skirt was placed over the frame. Small grommet holes were sewn into the mesh and secured with cotter pins and washers to metal pegs on the frames to prevent the net from disconnecting from the frame to minimize escapement. The traps were placed over the top of a redd and oriented to fully cover the egg pocket and as much of the tailspill as possible. The skirt was anchored into the substrate with 12 rebar posts, each 1-cm thick and 76-cm long. The rebar posts were pounded through grommets in the canvas skirt and cinched down using washers and hose clamps to prevent the skirt from rising. The exposed skirt material was then buried up to 30 cm in the substrate to prevent fry from escaping. Prior to installation, a plastic collection jar was attached to the funnel end of the trap to ensure that fry disturbed from the substrate during installation were captured. Once the trap was firmly installed, the collection jar was checked, and then reattached to the funnel end of the trap to capture any fry that emerged. The jar consisted of a 3.8 L polyethylene bottle with a 15-cm diameter funnel glued to the jar. Two holes were cut into the side of the jar and 0.32 cm nylon mesh was glued on top, allowing water to flow through to reduce salmon mortality in the jar (Figure 7).

Once traps were installed, they were checked 24 hours later, to look for fry that could have emerged prematurely due to the disturbance from trap installations. Thereafter, traps were checked three times weekly until projected peak emergence. Traps were checked more frequently during peak emergence (i.e., >100 fish when checked) to increase survival by reducing the time spent inside the collection jar. When emergence declined (i.e., ≤10 fish when checked), checks were reduced to twice weekly. Water temperature, turbidity, DO, water depth, and velocity at upstream and downstream ends of each trap were collected during each trap visit. Water temperature and DO were collected on the substrate surface with an YSI multi-probe Pro 2030. Turbidity was measured just below the water surface with a Hach 2100Q Portable Turbidimeter. Water velocity was measured at 60 percent of the water column depth with an OTT Hydromet MF-pro Water Flow Meter. During trap checks, each trap was cleared of debris and scrubbed with a bristle brush to remove organic matter. After cleaning, the collection jar was checked for any fry and other species. If fish were present, they were transferred into a bucket filled with water and brought to shore for processing. Salmon and non-salmonid species were sorted and placed into separate buckets to be processed. Salmon fry were counted, measured to fork length, and assigned a developmental stage. The assigned developmental stage corresponded to one of the following: stage 1 (egg); stage 2 (just hatched and translucent); stage 3 (fish has normal coloration and large yolk sac); stage 4 (fish beginning to absorb yolk); stage 5 (fish has fully absorbed yolk and is "buttoned up"); stage 6 (no seam). Caudal fin clips were taken from selected fry (up to 3 samples collected from each redd/week until a total of 15 samples/redd were taken) for genetic analysis to help determine parentage. After processing, fry were released downstream of the trap. Any non-salmonid species were identified, measured to fork length, and released downstream of the trap.

The initial timeline to remove the traps was January 31 to March 15, when each redd reached approximately 1,700 ATUs, the upper threshold when emergence ceased for previous fall-run emergence monitoring within the SJRRA (Castle et al. 2016a; Castle et al. 2016b). As in 2018, Reclamation conducted a Flow Bench Evaluation in 2019 to analyze the stability of conveyance, flow, and groundwater levels throughout the SJRRA to reduce the impact of seepage from increases in targeted Friant Dam releases (SJRRP 2018a; SJRRP 2014). The Flow Bench Evaluation in February 2019 resulted in an increase of Friant Dam flows from approximately 300 cubic feet per second (cfs) to 545 cfs (SJRRP 2019b). To avoid unsafe wading conditions and potential dislodging of emergence traps, all traps were removed by February 13. This resulted in the removal of the 12 trapped redds ranging between 1,399 and 1,758 ATUs, with four of the trapped redds still experiencing fry emergence. Removal involved placing a block net downstream of the trap to catch any fry or stray eggs that were released during the process. While the block net was set, a final trap check was performed and water quality measurements were taken. All the rocks covering the skirt were then removed, followed by removing the rebar. The emergence trap netting and frame were then lifted off the redd and carried to shore while two other crew members in dry suits monitored for eggs or fry dislodged during trap removal. After trap removal, staff from CDFW monitored the redd incubation habitat. Once completed, each redd was excavated to locate any remaining eggs and/or entombed alevins or fry. At the beginning of each excavation, a pole was placed at the start of the tailspill to signify the center of the redd. Excavation consisted of two crew members digging through the pit and tailspill to find the egg pocket(s) and any entombed fry. Eggs or fry dislodged from the egg pocket(s) were collected with dip nets and placed into containers to be counted. After no new eggs were encountered, width and depth of the egg pocket was recorded, as was the total area excavated. The redd was then backfilled with material from the surrounding riverbed.

Analysis

Mean daily temperatures were calculated during redd, carcass, and emergence surveys using 15-minute interval data from sensors at the CDEC FWQ, SJF, and H41 gages, when available. Temperature data from these gages were used in the ATU calculations for emergence trap installation and removal. Mean daily flows calculated from CDEC gages provide a measurement of water volume moving through the spawning grounds generally, although more localized information was obtained from field checks of water velocity upstream of each redd. As FWQ does not have a flow sensor, only two gages, SJF and H41, were used to calculate mean daily flows. Missing data from the H41 gage during November 1 to December 2, 2019, were replaced by mean daily temperatures from CDFW's nearby (2.4-rkm upstream of H41) Onset HOBO logger. The FWQ gage also recorded abnormally high temperatures in 2019 from October 9 to 23, thus mean daily temperature values from a nearby HOBO logger were substituted. Any remaining missing temperature and flow values from CDEC stations were linearly interpolated using the zoo package in R. Water temperature and flow measurements from CDEC gages were also used in the development of generalized linear models (GLMs) for emergence counts of redds (described below). See Durkacz et al.'s report (2019) for more details on 2018 temperature and flow data analysis, with the addition of mean daily temperatures from Reclamation – Friant Dam to replace missing H41 gage temperatures for October 20 to November 16, 2018.

Mean redd area was calculated for 122 of the 209 redds counted in 2019. Redd area was not calculated for the remaining 87 redds, because they were either superimposed or were part of a large redd congregation, making it difficult to obtain accurate measurements of individual redds. For redd congregations, length and width for the entire congregate were measured, but were not included within this analysis. Redd areas for the remaining 122 redds were calculated by multiplying length and width of each redd pit and tailspill then summing the pit and tailspill areas for each redd to provide the total redd area. The pre-redd mean sand composition, and pre-redd percent of each substrate type selected for 2017 to 2019 were calculated from available data.

Mobile monitoring detections suggested differences in spawning behavior between broodstock fish and volitional return and translocated fish. Mobile monitoring detections indicated that broodstock remained in holding habitat longer than natural returns. Whereas, natural return and translocated SRCS dispersed and were observed on large redds within spawning habitat. This suggested there were temporal differences in spawning activity and redd size. Mobile monitoring of acoustically tagged broodstock indicated that ≥ 50 percent of all broodstock detected in the holding habitat just below Friant Dam stayed there until October 3. To evaluate potential differences in spawn timing and redd size, redds were split into two groups by the date they were first detected. The first group of redds were detected from August 27 to October 3 and the second group of redds were detected from October 4 to November 15. Broodstock observed holding below the dam until October 3 were used to identify these periods. Mean redd area was calculated for all redds within each group for size comparison. We used a Welch *t*-test (which accommodates unequal variances and/or sample sizes between groups) to determine if there was a significant difference in mean redd size between the first and second group of redds for 2019. Redd areas were also compared across years between 2016 and 2019 using a nonparametric Kruskal-Wallis test.

To evaluate the influence of year, environmental factors, and redd characteristics on emergence count for 2018 and 2019 redds, we used an information theoretic approach (Burnham and Anderson 2002) to determine the relative fit of 21 candidate models. In particular, we were interested in using GLMs to assess the influence of nine predictor variables on fry emergence count: year of survey, surface DO, two different characterizations of water temperature during the incubation period (the mean of maximum temperatures identified for 10-day sliding windows, hereafter "10-day max temp", and the mean daily temperature), mean daily flow during incubation, and velocity measured just upstream of each individual redd. The four remaining predictor variables focused on characteristics of the redd, including tailspill depth (vertical distance between Original Streambed Surface and marker for Min D/V in Figure 5), the egg pocket height (vertical distance between Sample Marker and Egg Pocket in Figure 5), depth of the redd pit excavated (difference between Pit D/V and Pre D/V in Figure 5), and the percentage of redd surface composed of sand at time of detection. We excluded five emergence trapped redds from our model selection procedure, including two test redds during 2018, one redd of undetermined spawning status from 2019, and two redds from 2019 that were not excavated due to unsafe field conditions.

Prior to model selection, we calculated Pearson correlation coefficients for all pairs of predictor variables, and several were considered highly correlated ($r^2 > 0.70$). The inclusion of highly correlated covariates within the same regression can inflate variance and obscure relationships between modeled variables (see Dormann et al. 2013). Thus, because year was highly correlated with sand, DO, mean temperature, and mean flow, these covariates were not included within the same candidate models.

Throughout the analysis, the data were overdispersed with respect to a Poisson distribution, based on calculating a ratio of the residual deviance to the degrees of freedom greater than one (see Aho 2013). To account for overdispersion, negative binomial distributions with log link functions were fit. In certain cases, the number of observed cases of zero emergent fry exceeded the number of predicted cases, and hurdle models with a binomial zero-count process and a negative binomial positive-count process were applied. A hurdle model was chosen over a zeroinflated mixture model, because it was assumed that zeros observed at individual trapped redds were true structural zeros (i.e., not due to observation error but rather to failure to emerge; Martin et al. 2005). In addition, an outlier from a 2018 redd was determined to be influential to the regression, because the probability corresponding to the lower tailed F-distribution for Cook's distance exceeded 0.5 (see Aho 2013). Thus, a second set of models, with the outlier excluded, was also analyzed within the model selection framework.

All continuous data were standardized with a mean of zero and standard deviation of one to facilitate model fitting. Akaike Information Criterion with a correction for finite sample sizes (AIC_c) were calculated for the different candidate models to determine which set of predictors maximized the likelihood given the data, with more complex models penalized. Models with AIC_c < 2 were considered to have substantial support (Burnham and Anderson 2002), and those with $AIC_c > 2$ were not included within a model averaging process. Goodness-of-fit for each model was evaluated by graphing the residuals against fitted values and predictor values and ensuring no patterns (Zuur et al. 2009).

In addition to examining potential relationships between measured variables and emergence count, the ETF survival was estimated for 2018 and 2019 emergence trapped redds. The ETF survival is often defined as the proportion of eyed eggs within a redd that survive to emerge as fry from the substrate (Jensen et al. 2009). Here, ETF survival estimates for 2018 and 2019 were calculated as percentages, by dividing the average number of fry that emerged from all traps each year by the average fecundity. Fecundity for adult female SRCS that naturally return to the San Joaquin River is unknown. Thus, we used two different sources of fecundity estimates in the calculation of ETF survival: a) average fecundity from SCARF broodstock in 2018 (3,068 eggs) and 2019 (3,247 eggs), and b) Feather River Fish Hatchery natural hatchery returns in 2018 (5,523 eggs) and 2019 (4,558 eggs; P. Adelizi, CDFW, personal communication, 2020). Using these two different fecundity estimates established a range of ETF survival estimates for each year. This approach to calculating ETF survival assumes that all eggs deposited within redds are viable, fertilized, and successfully developed to the eyed stage.

Results

Snowpack in the San Joaquin Basin from several large storm events provided 141 percent of the normal unimpaired inflow to Millerton Lake from October 2018 to September 2019 and established a Wet Water Year allocation of Restoration Flows (SJRRP 2019a). Late storm events and flood flows terminated Adult Return Monitoring on May 21, 2019, while permitting SRCS to volitionally bypass barriers to access Reach 1 of the SJRRA. During spawning and emergence surveys, mean daily flow at SJF ranged from 347 to 447 cfs and 395 to 423 cfs at H41 with peak flows observed after storm events. Flows in 2019 were similar to 2018, except for peaks in the hydrograph in early February 2018 at H41 (Figure 8). In contrast to 2019, 2018 was designated a Normal-Dry Water Year for the Restoration Flow allocation. Mean daily temperatures ranged from 8.8 to 14.2°C at SJF, 8.9 to 14.3°C at FWQ, and 8.5 to 18.5°C at H41 (Figure 9). Temperatures from the Fresno County Sportsmen's Club to the Milburn Ecological Unit (corresponding to the H41 gage) were higher over the entire spawning assessment survey in 2019 than 2018. Temperatures at the H41 gage in 2019 approached or surpassed the upper critical spawning temperature (17°C) from August 27 to September 7, decreased below the lethal temperature threshold after September 7, and spiked back to near the upper lethal temperature on September 26 and 27 (SJRRP 2018b).

Redd Monitoring

In 2019, 209 redds and 9 test redds were detected in Reach 1 of the SJRRA (Figure 2). New redds were detected from September 10 to November 5, 2019 (Figure 10). Peak spawning activity was observed between September 24 and October 4. During this two-week period, 145 (69.4 percent) redds were documented (Figure 10). Temporal trends of spawning activity in the SJRRA during 2019 was similar to both 2017 and 2018 (Figure 10). However, field observations and mobile monitoring results (discussed below) suggest that hatchery return SRCS may have spawned earlier than broodstock. In 2019, 138 redds were detected from Friant Dam to Lost Lake and 71 redds were detected between Lost Lake and the Fresno County Sportsmen's Club (Figure 2). SRCS redd distributions from 2017 to 2019 were similar with the majority of redds created between Friant Dam and the Fresno County Sportsmen's Club in the SJRRA. However, no redds were documented below Highway 41 in 2019, although redds have been documented below Highway 41 in 2018 and previous fall-run surveys.

We documented 25 redds that exhibited superimposition (Figure 11). While only 25 redds were documented to have been superimposed, approximately 66 redds were observed between three distinct clusters (Figure 3). Clustered redds were not included within this evaluation, because we were unable to completely survey those areas without causing potential harm to the surrounding redds. Of the 25 superimposed redds, deposition was the most common form, with 18 (72 percent) of superimposed redds observed with substrate from a newly constructed redd deposited onto the pit or tailspill. Both deposition and scour were observed on 6 (24 percent) of the superimposed redds in 2019. One of the superimposed redds (4 percent) experienced only scour by a later spawning event. In total, superimposition increased from 9.5 percent in 2018 (Durkacz et al. 2019) to 12 percent in 2019.

Of the 209 redds, physical and environmental characteristics were measured for only 122 redds (Figure 11). The remainder were either too degraded to clearly identify redd features once spawners left or they were in clusters of redds that were not accessible without negatively affecting surrounding redds (Figures 2 and 3). In general, 2019 SRCS mean redd area (9.09 m^2) was larger than redds measured from 2016 to 2018 (Table 1). There was also a statistically significant difference among the redd areas for the four years compared ($\chi^2 = 49.14$, $df = 3$, $p < 0.001$); however, Dunn's test of multiple comparisons suggested that this difference was driven by 2019 redd areas being significantly larger than 2018 redd areas ($Z = -6.67$, adjusted $p < 0.001$), with no significant differences among other pairwise comparisons of years tested (Figure 12). Mean pit excavation depth of redds was 0.13 m in 2019, similar to 2016, 2017, and 2018 ($F = 1.23$, $df = 3$, $p = 0.30$). Mean pre-redd depth and mean pre-redd velocity were similar among survey years (Table 1).

In 2019, most spawning (54 percent) occurred where gravel was the dominant textural facie, similar to 2018 (Figure 13). However, only 18.8 percent of redds were constructed where cobble was the most dominant textural facie, unlike 2018, where 35.1 percent of redds were constructed in areas where cobble was the most dominant (Figure 13). Increased spawning in areas with a higher surface sand content was observed in 2019 (31.1 percent) than 2018 (8.1 percent) (Figure 13). Redd selection during 2019 was predominately within riffles (38.8 percent), runs (36.4 percent), and glides (23.0 percent) with only a small proportion detected in pools (1.9 percent; Table 2). The number of redds observed in glides during 2019 was much greater than that detected in 2017 or 2018 (Table 2).

Mobile Monitoring and Field Observations

In 2019, 47 acoustic tags were detected in the three survey reaches within the SJRRA. Of the SRCS detected, 42 were broodstock and the remaining 5 were translocated hatchery returns. Broodstock detections consisted of 24 May-release females, 11 May-release males, and 7 August-release females. Mobile monitoring detections of translocated hatchery returns included three males, one female, and one with an unknown gender. All detected translocated hatchery returns were released into Reach 1 of the SJRRA in May 2019. Acoustic detections were most prevalent (n =16) within the stilling basin just below Friant Dam. Generally, a maximum of four fish were detected in other areas at a given time.

Decreased broodstock detections after October 4 in the stilling basin below Friant Dam and smaller observed redds thereafter, lead to the hypothesis that average mean area of redds first detected after October 4 (group 2; 7.28 ± 4.02 m^2; mean ± 1 SD, n = 33) would be significantly smaller than that of redds detected prior to October 3 (group 1; 9.61 ± 5.83 m^2; mean ± 1 SD, ^{n} = 88). The results from a Welch two sample one-tailed t-test supported our hypothesis that mean redd area was significantly less for group 2 than group 1 (t = 2.50, df = 83.31, p = 0.015; Figure 14).

Carcass Survey

During 2019, 168 SRCS carcasses and one *Oncorhynchus mykiss* carcass that was likely a resident Rainbow Trout were recovered (SJRRP 2021). There were 123 carcasses recovered within the SJRRA from Friant Dam to Lost Lake, 41 from Lost Lake to the Fresno County Sportsmen's Club, and only 3 recovered from the Fresno County Sportsmen's Club to the Milburn Ecological Unit (Figure 4). The remaining SRCS carcass was recovered prior to the survey as a mortality in the James Bypass outside of the SJRRA. Of the carcasses recovered, 16 were broodstock, 3 translocated hatchery returns, and 149 volitional hatchery returns (Table 3). Broodstock carcasses (n = 16) included a sex ratio of 1:1.29 (M:F), and most (89 percent) females had fully spawned. Volitional hatchery return carcasses recovered (n = 147) included a sex ratio 1:2.42 of (M:F), with nearly all (92 percent) females fully spawned (Table 3). Mean fork length for volitional returns and translocated hatchery carcasses ranged from 111 to 246 mm larger than broodstock carcasses (Table 3, Figure 15).

Of the 168 SRCS carcasses recovered, 92 percent had clipped adipose fins and 91 percent were identified to have a CWT. Two of the 168 CWTs were lost during extraction and 15 weren't present or recovered for subsequent identification. The remaining 151 carcass CWTs consisted of three groups that either migrated into SJRRA (volitional hatchery return, *n* = 133), were captured and released into the SJRRA (translocated, *n* = 3), or were released directly from SCARF into the SJRRA (broodstock, *n* = 14). All recovered volitional hatchery return and translocated carcasses were brood year 2016, released in 2017 below fish passage barriers for reintroduction. The remaining 14 broodstock consisted of two brood years; five were brood year 2016, and nine were brood year 2015, both of which were released into Reach 1 of the SJRRA in 2019. The introduction method to the SJRRA of the last remaining carcass recovered is unknown because it was recovered as a skeleton. However, the CWT indicated it was from brood year 2016 (Table 4).

From the carcasses recovered, 83 percent were age-three, 5.4 percent are age-four, and the remaining 10.7 percent were unknown because CWTs were missing or lost during extraction. The age-four carcasses were from adult broodstock releases. Both volitional and translocated returns with CWTs were all age-three. All of the carcasses recovered were identified as fish that originated from SJRRP, indicating that there were no strays detected within Reach 1 of the SJRRA.

Emergence Survey

In 2019, a total of 8,424 fry were observed in the twelve trapped redds; 675 were mortalities (Table 5). Mean emergence per trap was 702 fry in 2019, 25.5 times greater than 2018 when mean fry emergence was only 27.5 per redd (Table 5, Figure 16). The percentage of mortalities per redd, when weighted by the number of emergent fry, was also lower in 2019 (8 percent) than in 2018 (20 percent). During the 2019 survey season, the epoxy adhering the collection jar together failed on four emergence traps and the collection jar was lost during peak emergence. Three of these losses occurred at redds exposed to the highest water velocity flows. Therefore, emergence for these traps is likely underestimated. Both trapped redds NR12SR19 (rkm 418) and NR189SR19 (rkm 429) had the lowest number of emerging fry with just one emerged fry each, and in both cases emerged fry were mortalities. The mean fork length (FL) for all emerged fry was similar for 2019 (33.4 ± 4.3 mm; mean ± 1 SD) and 2018 (34.1 ± 2.4 mm; mean ± 1 SD) (Table 5). However, in 2019 the range of fry sizes (18 to 56 mm) was larger than 2018 (28 to 39 mm). Of the 8,424 fry that emerged, 68.7 percent were classified as stage 5 in their development, 28.3 percent were stage 4, and 2.7 percent comprised stages 2 or 3. Fry classified as stage 6 were the least abundant, 0.25 percent. Upon excavation, unhatched eggs were recovered from 60 percent of the 10 redds suitable for excavation (Table 5). We did not excavate NR12SR19 and NR128SR19 (rkm 423), as they were either too deep or high velocity which prevented safe excavation. The mean number of eggs recovered per redd was 40 in 2019, with more than 80 percent coming from just one trap (NR189SR19). The mean number of eggs recovered (152) in 2018 was 3.8 times higher than in 2019 (39.8). Redds that did not have emergence or eggs upon excavation were excluded while calculating the mean number of eggs per redd because they were assumed to be test redds.

In 2019, mean start of emergence was at 784 ATUs (range 631 to 1,177 ATUs) and ended at a mean of 1,318 ATUs (range 972 to 1,630 ATUs). As a function of ATUs, emergence started earlier and ended later in 2019 than 2018. This was also reflected in the duration of emergence, with a longer duration in 2019 (1 to 81 days, mean 46 days) compared to 2018 (1 to 37 days, mean 14 days; Table 5). Fish caught near the end of the sampling season tended to be larger and more developed (stage 5 and 6) than the average emergence size, possibly due to the emerged fry holding inside the trap or holding longer in the substrate. However, due to the early removal of the emergence traps in 2019, ten of the twelve trapped redds did not reach 1,700 ATUs before being removed. However, six of these ten traps were no longer capturing fry. The remaining four trapped redds had fry captured during the last trap check, before trap removal and excavation, and early removal may have resulted in an underestimation of ETF survival.

Patterning in the residuals versus environmental predictors and fitted values indicated poor GLM fits that were not remedied with transformations, perhaps due to unaccounted for predictors and/or limited sample size. Thus, it should be emphasized that results from the GLM analysis are considered very preliminary. With these caveats in mind, according to the 21 GLMs assessed, the best approximating candidate model for predicting fry emergence contained only year as a predictor for fry emergence based on the data with the 2018 redd outlier removed (Table 6). The model with both year and pit excavation depth of redds had the second greatest Akaike weight and was the only other model within $\Delta AIC_c < 2$. However, the comparatively lower AIC_c value for this more complex version of the better performing model with only year indicates no additional information is gained through the inclusion of pit excavation depth of redds as a predictor. Of the environmental variables included within the model selection procedure, DO, mean temperature, proportion of sand, and mean flow all yielded Akaike weights below 0.001 (Table 7). When the influential outlier (NR33SR18) was included in analysis, two models performed better than the model with year only, based on AIC_c scores. The model with pit excavation depth of redds and year as predictors and the model with velocity upstream of the redd and year as predictors both slightly improved model fit to emergence counts compared to the model with year as the only predictor. All three models were within $\Delta AIC_c < 2$ (Table 8). AIC_c values for models based on the inclusion of the outlier increased compared to those for models without it, lending support for model prediction based on outlier exclusion. Table 9 provides statistical results based on the top model of year as the predictor for fry emergence, showing that compared to year 2018, 2019 is associated with a log increase in emergence count of 5.17, equivalent to approximately 175 more emergent fry.

Given the poor GLM fits of emergent fry per redd to several recorded environmental factors (water temperature, DO, water velocity, and pre-redd surface fraction of sand), quantitative predictions of fry count from environmental variables were not developed. However, collinearity between year and these same variables suggests that year may in part be acting as a broader alias for environmental conditions by year that affect emergence (Figures 16, 17, 18, 19, 20, and 21, and results within Tables 6-8). For this reason, we further explored differences by year during the incubation and emergence season in water temperature, DO, turbidity, water depth, velocity, flow, and percentage of sand at emergence trapped redd sites. Based on spot checks at individual trapped redds (see Table 9), water temperatures during both 2018 and 2019 were within the optimal incubation temperature threshold (< 13°C; Figure 17) for SRCS (SJRRP 2010, Beer and Anderson 2001). Mean and maximum water temperatures calculated from nearby, continuously monitored CDEC gages were generally higher than water temperatures from spot checks (compare Figures 17 and 18 for mean temperatures). Maximum temperatures recorded during the incubation period reached 16.8°C at two redds. Mean redd temperatures based on CDEC gages were significantly different by year based on a Welch two sample *t*-test ($t = 5.08$, $df = 14.00$, $p < 0.001$), with higher temperatures (albeit, still within the optimal range) during the incubation and emergence season in 2018 than 2019 (Figure 18). Surface DO was lower in 2018 than in 2019 ($t = -8.83$, $df = 12.04$, $p < 0.001$; see Table 10 and Figure 19). At every trapped redd in 2019, mean DO exceeded 10 milligrams per liter (mg/L), while for 2018 DO was less than 10 mg/L at trapped redds (Table 9). Mean depth (upstream and downstream of the redd) and mean turbidity in 2019 were similar to their corresponding values in 2018 (Table 10). While mean turbidity measured at NR03SR19 (4.9 NTU) exceeded the relatively low mean (2.3 NTU) and range (2.0 to 2.6 NTU) measured at other traps, the difference in turbidity was not biologically meaningful (Table 9; Newcombe and MacDonald 1991). Velocities (upstream and downstream of emergence trapped redds) were also similar between the two years (Table 10; Figure 20), and a statistical analysis of year-specific upstream velocities (presumably the more biologically-relevant of the two velocity measurements for emergence success) confirmed this result (t = -1.02, df = 13.27, p = 0.33). However, nonparametric analysis based on calculations from more continuous, but less spatially-localized measurements of CDEC gage flow characterized mean flow as significantly higher for emergence trapped redds in 2018 than in 2019 ($\chi^2 = 11.13$, $df = 1$, $p < 0.001$). This higher mean flow during the 2018 incubation and emergence season compared to 2019 may be linked to the rain event that peaked the hydrograph over 500 cfs in early February (Figure 8). Similar to findings from the redd survey, the fraction of sand adjacent to emergence trapped redds was significantly lower in 2018 than in 2019 ($\chi^2 = 11.18$, $df = 1$, $p < 0.001$; Figure 21).

In 2019, the average fecundity of broodstock SRCS (3,247 eggs) spawned at the SCARF and average fecundity of natural return SRCS (5,523 eggs) spawned at the FRFH were used to calculate ETF survival. Egg-to-fry survival estimates were from 12.7 to 21.6 percent for 2019, compared to substantially lower ETF survival for 2018 (0.60 to 0.90 percent) (Table 11). The lower value for ETF survival in each year's range is based on using the average SRCS fecundity from FRFH naturally returning adults.

Discussion

In 2019, nearly a five-fold increase in SRCS redds in Reach 1 of the SJRRA was observed from the previous season. This increase was preceded by the volitional return of adult SRCS to the SJRRA. Spawning during 2019 was similar both spatially and temporally to historical trends for SRCS in the San Joaquin River (Yoshiyama et al. 2001, Williams 2006). However, lethal spawning temperature (17°C) at H41 during the onset of the 2019 redd monitoring and carcass surveys may have influenced spawning habitat selection and restricted the spatial distribution of redds to the 17 rkm below Friant Dam, where water temperatures are generally cooler than elsewhere in the SJRRA (SJRRP 2018b). In 2019, Spring-run Chinook Salmon selected similar spawning areas that were used in 2018. Of the 209 redds, the largest proportion (66 percent) were distributed in the 4 rkm directly downstream of Friant Dam. The remaining 34 percent were distributed in the 13 rkm downstream of Lost Lake. The spatial distribution of SRCS redds from 2016 to 2019 suggests that the most suitable spawning habitat may be restricted to the 17 rkm directly downstream of Friant Dam. To accomplish SJRRP goals, continued investigation of spawning activity is crucial to identify which physical and environmental variables affect spawning site selection. Managing Reach 1 water temperatures through Restoration Flows and cold-water pool releases, coupled with gravel augmentation, may be the first steps needed to help create more suitable spawning habitat in support of SRCS natural spawner abundance and juvenile production goals.

Superimposition was greater in 2019 than 2018 (12 versus 9.5 percent). However, superimposition may have been underestimated in 2019 because areas with clustered redds were unable to be completely surveyed without potential harm to surrounding redds. Therefore, the number of redds, including superimposed redds, may have been undercounted. These clustered redds were located above Friant Bridge (rkm 439), above the hatchery outflow (rkm 428) in the main river channel, and in the Lower Willow Riffle (rkm 420) (Figures 2 and 3). The Fisheries Framework sets a target that superimposition of fall-run Chinook Salmon on SRCS redds be less than 10 percent (SJRRP 2018b). However, superimposition is already occurring at >10 percent for SRCS spawning in the SJRRA with relatively low population numbers compared to the Restoration Goal objectives. McNeil (1964) indicated a corresponding increase in egg mortality with increasing spawner density, primarily caused by superimposition. Higher rates of egg mortality within the SJRRA could also become an issue if rates of superimposition increase.

Previous studies have shown that superimposition increases as the density of spawners increase and have been attributed to limited spawning habitat (McNeil 1964; Weeber et al. 2010). Since more than 10 percent of redds are shown to exhibit superimposition, suitable spawning habitat may be a limiting factor within the SJRRA. However, as a counter point, ETF survival rates were lower in the year with lower superimposition, so other factors are also important in determining survival.

In addition to higher rates of superimposition with a greater number of spawners, redds in 2019 had a larger mean area than those of the previous years (Figure 12). We hypothesize this is attributed to the larger size of the natural returning hatchery SRCS spawning within the SJRRA. Mean redd area may increase when there is a large proportion of natural returns and may subsequently reach the average redd size (12.0 m^2) observed during previous fall run surveys (Castle et al. 2016a, Castle et al. 2016b). The Fisheries Framework (SJRRP 2018b) suggests that 270,000 m^2 of suitable spawning habitat for SRCS could sustain 22,500 spawning females if redds were 12 m^2. The observed mean redd area can also help inform the quantification of needed spawning habitat area for the reestablishing population. Based on temperature thresholds for incubation and emergence (Gordon and Greimann 2015; SJRRP 2018b), the first 8 to 11 rkm below Friant Dam for most Water Year types have water temperatures suitable for Chinook Salmon to successfully spawn and produce viable offspring. Modeling suggests the first 8 rkm downstream of Friant Dam provides approximately 53,000 m^2 of spawning habitat that is thermally and hydraulically suitable to Chinook Salmon (see Gordon and Greimann 2015), therefore capable of supporting up to 4,417 spawners. The SJRRP has set a long-term (i.e., beyond 2040) SRCS abundance target of 22,500 spawning females with redd sizes of 12 m^2. If this abundance target was reached under current conditions, there would be a 217,000 m^2 deficit in suitable spawning habitat if average redd size reaches 12 m^2. Average redd size for SRCS in 2019 was 9.09 m^2. If redd size remains consistent with the 2019 values, an additional 151,525 m^2 of suitable spawning habitat would be needed to reach the long-term abundance target of 22,500 spawning females. Higher rates of superimposition and known habitat availability suggests that there may be greater competition for suitable spawning habitat as the number of spawners increase and redd sizes may increase. This suggests there may be a future need to create a minimum of 151,252 m^2 of suitable spawning habitat. This may be accomplished through gravel augmentation and mechanical mixing of the bed material (Meyers 2019).

The quality, quantity, and relative size of spawning gravel can limit available spawning habitat and spawning success of Chinook Salmon (Kondolf 1993). In the SJRRA, the most dominant surface textural facies at SRCS spawning sites in 2019 were gravel, sand, cobble (in descending order). In 2019, spawning adult SRCS constructed redds in habitats that had an average of 12.8 percent more sand than in 2018. However, because these are only surface assessments of sand composition upstream of redds, our surveys may not fully reflect sand accumulation within redds. SRCS also constructed 24.9 percent of redds in glides and pools in 2019, while no redds were documented within this habitat type in 2018. This shift in spawning habitat selection for areas with slightly higher concentrations of sand, within pools and glides may indicate that SRCS were restricted to less optimal spawning habitat due to greater spawner densities or because of differences in river flow and flow releases in 2019 (Hughes and Murdoch 2017). However, since the SJRRP is still in the Recolonization Phase, the quantity and quality of suitable spawning habitat within the SJRRA is not well known; therefore, we cannot conclusively say that increased spawner density or variation in river flows is the cause for selecting alternative spawning habitat in 2019.

We had difficulty determining the spawner identity (i.e., volitional hatchery return, translocated hatchery return, or broodstock) for each redd in 2019. Most spawning occurred across two survey weeks and many redds were clustered together, prohibiting individual identification. In the future, identifying individual spawners may be improved by using floy tags with bright contrasting colors, which indicate distinct release groups. In 2019, translocated and volitional hatchery return fish were larger on average than broodstock and natural returning fish may have produce larger redds. Prior to broodstock leaving the holding habitat near Friant Dam, the mean area of measured redds were significantly larger than that measured after broodstock movement to the spawning grounds. Other studies have shown similar results, finding that redd size is related to fish size and Chinook Salmon that spawn earlier are generally larger and produce larger redds (Burner 1951, Ottaway et. al, 1981, Neilson and Banford 1983). Hughes and Murdoch (2017) suggest even a short time of juvenile rearing in a hatchery may be associated with a reduction in redd size and excavation depth. Consequently, broodstock/hatchery-reared redds could be more susceptible to mortality because of hydraulic scour, egg loss, and deleterious effects from superimposition (DeVries 1997). Results from the SJRRP suggest that broodstock tend to be smaller than volitional return SRCS, and broodstock may produce smaller redds than volitional returns. There may be interaction between the variables contributing to redd size. However, current data suggests that an extended time in a hatchery (as exhibited by broodstock released as adults) may be associated with a reduction in redd size. Although our preliminary method showed a significant difference in mean redd area between groups delineated by time in the SJRRA, further investigation is needed to determine the extent to which broodstock spawn later and/or create smaller redds than natural returns, and any corresponding effects on ETF survival.

Recovered carcasses had a similar distribution to redds in 2019. Zhou (2002) demonstrated that larger carcasses are more likely to be detected during carcass surveys, which may have resulted in a greater proportion of the larger volitional returns being recovered than broodstock because of size selective bias. For this study, females represented the largest proportion of SRCS carcasses recovered. Studies on SRCS by Murdoch et al. (2009) suggested that sexually dimorphic behavior may result in the recovery of more female than male SRCS carcasses. They suggested that behavior of female SRCS generally includes the construction of a redd and nest guarding until senescence, while males may spawn with multiple females but begin to drift downstream when their energy is depleted. In the SJRRA deep pools are common below spawning riffles which may have made it more difficult to recover downstream drifting male SRCS carcasses. The deepest and most prevalent pools are located below spawning riffles from Lost Lake to the Fresno County Sportsmen's Club, likely contributing to the lower proportion of carcasses recovered in this area. The low numbers of translocated hatchery return and broodstock SRCS carcasses recovered limited our ability to document how successful both groups were able to fully spawn. Genetic analysis of tissue samples collected from emergence trap fry, recovered carcasses, and juveniles collected with rotary screw traps are still in progress. Results from genetic analyses will identify the parentage of progeny that were successfully produced by SRCS and elucidate spawning success for each type of spawner.

Mean fry emergence was 25.5 times greater in 2019 than 2018, and 2019 was associated with higher DO, lower temperature, and lower flow. Similarly, the mean juvenile SRCS captured in rotary screw traps were 23.5 times greater in 2019 than 2018 (Z. Sutphin, Reclamation, personal communication, 2021; Hutcherson et. al 2020). Emergence trap and rotary screw trap surveys suggest that juvenile production and survival was over 20 times greater in 2019 than 2018, assuming capture efficiency was similar between years. Continued emergence monitoring with more traps per year will enable a quantification of the environmental effects, if present, given the range of environmental DO in the river and redds. Mean DO values for both 2018 and 2019 exceeded the Fisheries Management Plan objective for dissolved oxygen greater than 6 mg/L when

Chinook Salmon are present (SJRRP 2010). It should be noted that DO values presented herein are based on benthic surface measurements, whereas hyporheic measurements of dissolved oxygen in the SJRRA could be lower than corresponding surface values (Nelson and Reed 2014). Similarly, lower temperatures (evaluated from nearby continuous CDEC gage measurements during the incubation period) may also have aided greater fry emergence in 2019 than in 2018. More local continuous measurements of surface water temperature, or ideally of hyporheic water temperatures of the incubation environment may aid inference about thermal effects on emergence count. Based on statistical analysis, gage-measured mean flows at trapped redds were higher in 2018 than 2019. However, this result may not represent a biologically-relevant difference in flows for emergence; the higher mean flow in 2018 may be primarily linked to the February peak in the hydrograph at the end of the 2018 survey, after peak emergence. As additional support, no difference was found in point measurements of velocity adjacent to trapped redds by year. Moreover, as with temperature monitoring, continuous, hyporheic measurements of intragravel flow from CDFW's incubation habitat study (results forthcoming) will greatly assist with an understanding of the effects of the SJRRA habitat conditions on emergence success.

Although more favorable environmental conditions such as increased DO and reduced mean temperatures may have helped support greater emergence counts in 2019 compared to 2018, the large difference in ETF survival may also be connected to spawner identity. As previously mentioned, the number of spawners in 2019 contributing to the spawning population was higher consisting primarily of volitionally-passed, hatchery returns, in contrast to the lower number of predominantly broodstock spawners in 2018. Linking individual redds to spawner group identity (e.g., distinguishing redds produced by volitionally passed and translocated hatchery returns versus broodstock released spawners) is needed to better understand the role of spawner characteristics in determining ETF survival and the utility of releasing excess broodstock spawners as a reintroduction strategy. Stark et al.'s research (2018) determined that egg viability (survival until the eyed egg stage) was significantly greater for wild-origin versus captive-reared SRCS in East Fork Salmon River, Idaho.

We also observed a lower weighted average number of mortalities per redd in 2019 (8 percent) than 2018 (20 percent) and the majority of 2019 fry mortality occurred in the emergence trap on redd NR03SR19. We hypothesize the mortality was induced by trap placement. The NR03SR19 trap was placed at a slight angle to the direction of flow which caused the thalweg within the trap to flow into the side of the trap instead of the catchment jar. As a result, some of the emerging fry were impinged on the side of the trap in two different places. For future emergence studies, orientation of traps will be verified to help reduce the risk of incidental mortalities. Additionally, we encountered issues with the fish catchment jars. The glue used to fabricate the jars became brittle in the cold water and failed, resulting in the loss of the jar during peak emergence on four of the trapped redds (NR03SR19, NR12SR19, NR43SR19 and NR128SR19). Thus, our emergence counts and ETF survival from these traps may be underestimated. To reduce glue failure, alternative marine epoxy will be used to help prevent jar losses in future emergence studies. However, to maximize efficacy, the emergence trap jars could be redesigned with a threaded collar attachable with a hose clamp and threaded jar that screws directly into the collar. Preventing jar failure or an improved jar design will help SJRRP gain more accurate ETF survival estimates and inform future habitat improvement like gravel augmentation.

Generally, high concentrations of fine sediment in the incubation environment can reduce gravel permeability and hyporheic flow, which can lead to lower DO, and result in early emergence, entombment, or mortality during incubation and emergence (Chapman 1988; Frassen et al. 2012). Previously, developmental stages have even been used to indicate the health of emerging fry and habitat quality (Kondolf et al. 2008). Under ideal conditions, or conditions with hyporheic upwelling and high DO, salmon typically emerge with their yolk sac fully absorbed (stage 5), whereas in areas with higher concentrations of fine sediment, it was noted that many fry emerged without fully absorbing their yolk sac (stage 4 and under; Cardenas et al. 2016; Tappel and Bjornn 1983). Since surface pre-redd sand content was more prevalent and the second most dominant textural facie within selected spawning areas in 2019, it may have been a factor that contributed to the 31 percent of fry that emerged at stage 4 and below. Eggs were found at six of the ten redds that were excavated after emergence trap removal. All redds in 2019 were verified as “true redds” by the emergence of fry or eggs detected during redd excavations. Eggs were less abundant during redd excavations in 2019 than 2018. We suggest that the discovery of fewer eggs in 2019 may be due to greater ETF survival and emergence success, as demonstrated by the overall increase in fry emergence observed in 2019.

In 2019, SRCS fry emerged at similar ATUs to what has been documented for fall-run Chinook Salmon in the SJRRA from prior emergence studies (Castle et al. 2016a; Castle et al. 2016b). Similar emergence timing of fall-run and SRCS captured during 2019 suggests most emergence still occurs between 650 and 1,700 ATUs for SRCS. Similarities in emergence timing between fall-run and SRCS show that the use of ATU's is still a successful method for predicting emergence timing. In the future, scheduling bench flow evaluations later in the spawning season would allow this study to complete the surveying of redds constructed at tail of the season and remain trapped until after 1,700 ATU's or emergence has subsided for all traps being surveyed. This would allow the SJRRP to capture a higher percentage of emerging fry to provide a more accurate range of emergence timing based upon ATU's and to gain a more accurate estimate of ETF survival. Multiple years of emergence trapping data will help us improve our understanding of emergence timing and ETF survival under varied temperature regimes and Water Year types.

Fry captured in 2019 included a wider range of larger sizes (fork length) than fry observed in 2018. While measuring fry in 2019, exogenous feeding on mayfly nymphs within the traps was observed. Larger fry were primarily captured in emergence traps exposed to lower water velocity, where fry were observed holding within the pit of these redds upon trap removal. This suggests that fry may have been able to avoid being captured in the collection jars of these traps, swimming freely, and foraging on colonized macro-invertebrates. Capture avoidance and prey availability may explain why fry in these traps were able to grow larger.

Prior studies have shown that higher fine sediment composition can reduce ETF survival of salmonids (Chapman 1988, Franssen et al. 2012, Meyers 2019, Sear et al. 2008), which may have contributed to the poor ETF survival observed within SJRRA (Shriver et al. 2015b, 2016). However, our current assumptions for ETF survival may overestimate fecundity, fertilization rates, egg viability, and survival to the eyed egg stage, which may result in underestimates in ETF survival. If the assumptions are true, ETF survival was still lower than SJRRP survival goals. The abundance of fine sediments in the San Joaquin River is well documented and exists due to a multitude of activities and processes including mining, Friant Dam construction, erosion, and streambed widening (Williams and Wolman 1984; Williams 2006). Dams generally alter flow regimes, reduce sediment transport, and prevent gravel replenishment necessary for suitable salmonid spawning habitat. After dam construction, fine sediment can also accumulate within the streambed downstream due to flow restrictions (Kondolf 1997). Fine sediment accumulation can reduce the hyporheic water replenishment rate and result in lower available DO than is necessary for developing salmon embryos, by preventing the expulsion of waste products and entombing fry, leading to higher mortality (Chapman 1988, Meyers 2019). Sediment accumulation within the redds of the SJRRA may be contributing to reduced fry emergence. Future emergence studies focused on sampling the sediment composition and the physical environment within redds are needed to determine which factors influence ETF survival.

Bowerman et al. (2014) have shown that survival of salmonids from the eyed egg to the fry stage is < 40 percent when fine sediment composition is > 20 percent. The relatively high composition of sand (mean 34.8 percent, and range 0 to 80 percent) observed in the pre-redd area within the SJRRA may be impacting in-river production and necessitate habitat restoration to reach SJRRP's goals of ≥ 50 percent ETF survival (SJRRP 2018b). Patterning in the residuals of the GLMs relating percentage of pre-redd sand to emergence prevented drawing conclusive results on the effects of sand on ETF survival. In addition, greater emergence coincided with 2019 when trapped redds were associated with a greater proportion of sand compared to 2018. However, the greater ETF survival for 2019 may be related to spawner identity (i.e., more productive natural returners vs. less productive broodstock) more so than sand composition. We suggest that continued data collection and increases in natural returns to the SJRRP population will provide a better understanding of the relative role of each in emergence success. In addition to emergence traps, studies with egg tubes in artificial redds may provide more accurate rates of survival from the green egg stage (just after fertilization) to the eyed egg stage. These calculations of early life survival could be used to further improve our calculated estimations of ETF survival rates from emergence traps. ETF survival estimates from emergence traps are currently obtained by dividing emerged fry by female fecundity estimates, thus assuming all eggs are viable and fertilized. In addition, prior studies have shown increased fine sediment deposition within emergence traps, which may cause entombment and reduce ETF survival (Reiser et al. 1998). To determine if emergence traps are contributing to reduced ETF survival, future evaluations of potential emergence trap affects are ongoing.

For 2018 and 2019, CDFW has continually collected substrate samples and incubation habitat data of redds in the SJRRA (Shriver 2015b, 2016). However, analysis of these data are currently pending. This effort to assess data collected during redd and emergence surveys, coupled with CDFW's substrate samples and spawning incubation data will help the SJRRP identify a need for improving spawning habitat quality within the SJRRA. The application of results from these and other monitoring studies can guide restoration actions and an adaptive management program that aids the reintroduction of SRCS to the San Joaquin River.

References

Aho, K. A. 2013. Foundational and applied statistics for biologists using R. Chapman and Hall/CRC.

Beacham, T. D., and C. B. Murray. 1990. Temperature, egg size, and development of embryos and alevins of five species of Pacific salmon: a comparative analysis. Transactions of the American Fisheries Society 119:927–945.

Beer, W. N., and J. J. Anderson. 2001. Effect of spawning day and temperature on salmon emergence: interpretations of a growth model for Methow River Chinook. Canadian Journal of Fisheries and Aquatic Sciences 58(5):943-949.

Berejikian, B. A., J. T. Gable, and D. T. Vidergar. 2011. Effectiveness and trade-offs associated with hydraulic egg collections from natural salmon and steelhead redds for conservation hatchery programs. Transactions of the American Fisheries Society 140:549–556.

Bowerman, T., B. T. Neilson, and P. Budy. 2014. Effect of fine sediment, hyporheic flow, and spawning sit characteristics on survival and development of bull trout embryos. Canadian Journal of Fisheries and Aquatic Sciences 2014, 71(7):1059-1071.

Buffington, J. M., and D. R. Montgomery. 1999. A procedure for classifying textural facies in gravel-bed rivers. Water Resources Research 35(6):1903-1914.

Burner, C. 1951. Characteristics of Spawning Nests of Columbia River Salmon. Fishery Bulletin 61. Fishery Bulletin of Fish and Wildlife Service 52. U.S. Department of Interior. U.S. Fish and Wildlife Service.

Burnham, K. P., and D. R. Anderson. 2004. Model selection and multimodel inference: a practical information-theoretic approach. Second Edition. Springer.

Cardenas, M. B., A. E. Ford, M. A. Kaufman, A. J. Kessler, and P. L. M. Cook. 2016. Hyporheic flow and dissolved oxygen distribution in fish nests: The effects of open channel velocity, permeability patterns, and groundwater upwelling. Journal of Geophysical Research: Biogeosciences 121:3113–3130.

Castle, C., J. N. Cullen, J. Godwell, Z. Johnson, M. Workman, J. Kirsch, and A. Shriver. 2016a. Fall-run Chinook Salmon spawning assessment during 2013 and 2014 within the San Joaquin River, California. Annual Technical Report of the San Joaquin River Restoration Program. U.S. Fish and Wildlife Service, Lodi, California.

Castle, C., J. Barkstedt, J. Kirsch, and A. Shriver. 2016b. Fall-run Chinook Salmon spawning assessment during 2015 within the San Joaquin River, California. Annual Technical Report of the San Joaquin River Restoration Program. U.S. Fish and Wildlife Service, Lodi, California.

California Department of Fish and Wildlife (CDFW) 2019. Annual Report of Broodstock Activities. San Joaquin River Restoration Program.

Chapman, D. W. 1988. Critical review of variables used to define effects of fines in redds of large salmonids. Transactions of the American Fisheries Society 117:1–21.

DeVries, P. 1997. Riverine salmonid egg burial depths: review of published data and implications for scour studies. Canadian Journal of Fisheries and Aquatic Sciences 54:1685–1698.

Dormann, C. F., J. Elith, S. Bacher, C. Buchmann, G. Carl, G. Carré, J. R. G. Marquéz, B. Gruber, B. Lafourcade, P. J. Leitão, T. Münkemüller, C. Mcclean, P. E. Osborne, B. Reineking, B. Schröder, A. K. Skidmore, D. Zurell, and S. Lautenbach. 2013. Collinearity: A review of methods to deal with it and a simulation study evaluating their performance. Ecography 36(1):27–46.

Durkacz, S., L. Smith, L. Yamane, A. Demarest, A. Raisch, and A. Shriver. 2019. 2018 Spring-run Chinook Salmon spawning assessment within the San Joaquin River, California. San Joaquin River Restoration Program Annual Technical Report. U.S. Fish and Wildlife Service, Lodi, California.

Fisher, F. W. 1994. Past and present status of Central Valley Chinook salmon. Conservation Biology 8:870–873.

Franssen, J., C. Blais, M. Lapointe, F. Bérubé, N. Bergeron, and P. Magnan, 2012. Asphyxiation and entombment mechanisms in fines rich spawning substrates: experimental evidence with brook trout (*Salvelinus fontinalis*) embryos. Canadian Journal of Fisheries and Aquatic Sciences 69(3):587–599. doi:10.1139/f2011-168.

Fry, D. H. 1961. King salmon spawning stocks of the California Central Valley, 1940-1959. California Department of Fish and Game 47(l):55-7l.

Gallagher, S. P., P. K. J. Hahn, and D. H. Johnson. 2007. Redd counts. In D. H. Johnson (Ed.), Salmonid field protocols handbook: Techniques for assessing status and trends in salmon and trout populations. pp. 197–234. Bethesda, MD: American Fisheries

Galloway, D., and F. S., Riley. 1999. San Joaquin Valley, California. Land Subsidence in the United States: U.S. Geological Survey Circular 1182:23–34.

Gordon, P. E., and B. P., Greimann, 2015. Preliminary Investigation of Spawning Habitat Within Reach 1 of the San Joaquin River. San Joaquin River Restoration Program.

Hughes, M., and A. Murdoch. 2017. Spawning habitat of hatchery Spring Chinook Salmon and possible mechanisms contributing to lower reproductive success. Transaction of the American Fisheries Society. 146(5):1016-1027.

Hutcherson, J., Z. Sutphin, P. Ferguson, M. Grill, J. C. Garza, and A. Clemento. 2020. Juvenile Spring-Run Chinook Salmon Production and Emigration in the San Joaquin River Restoration Area. 2018-2019 Monitoring and Analysis. San Joaquin River Restoration Program Annual Technical Report. Bureau of Reclamation, Denver Technical Services Center.

Jensen, D. W., E. A. Steel, A. H. Fullerton, and G. R. Pess. 2009. Impact of fine sediment on egg-to-fry survival of Pacific Salmon: a meta analysis of published studies. Reviews in Fisheries Science. 17(3):348–359.

Kondolf, G. M. 1997. Hungry Water: Effects of dams and gravel mining on river channels. Environmental Management 21(4):533–551.

Kondolf, G. M., M. G. Wolman. 1993. The Sizes of Salmonid Spawning Gravels. Water Resources Research. Vol. 29 No. 7. Pages 2275-2285

Martin, T. G., B. A. Wintle, J. R. Rhodes, P. M. Kuhnert, S. A. Field, S. J. Low-Choy, A. J. Tyre, and H. P. Possingham. 2005. Zero tolerance ecology: Improving ecological inference by modelling the source of zero observations. Ecology Letters 8(11):1235–1246.

McNeil, W. J. 1964. Redd superimposition and egg capacity of pink salmon spawning beds. Journal of the Fisheries Board of Canada 21:1385-1396.

Meyers, M. A. 2019. Artificial Redd Study: The effect of sand accumulation on incubation habitat quality. San Joaquin River Restoration Technical Memorandum. California Department of Water Resources, Fresno, California.

Murdoch, A. R., T. N. Pearsons, and T. W. Maitland. 2009. Use of carcass recovery in evaluating the spawning distribution and timing of spring Chinook Salmon in the Chiwawa River, Washington. North American Journal of Fisheries Management 29:1206-1213.

Natural Resources Defense Council (NRDC) vs. Rodgers. 2006. Stipulation of Settlement. U.S. District Court, Eastern District of California (Sacramento Division), Case No. CIV-S-88-1658 LKK/GGH.

Neilson, J. D., and C. E. Banford. 1983. Chinook Salmon (*Oncorhynchus tshawytscha*) Spawner characteristics in relation to redd physical features. Canadian Journal of Zoology 61 (7):1524-1531.

Nelson, S. M., and G. K. Reed. 2014. Continuous Monitoring of Dissolved Oxygen, Conductivity, and Temperature in Surface Water and Hyporheic Zone Water in the San Joaquin River below Friant Dam During the 2012-2013 Salmon Spawning Period. Denver, Colorado.

Newcombe, C.P. and D.D. MacDonald. 1991. Effects of suspended sediments on aquatic ecosystems. North American Journal of Fisheries Management 11:72-82.

Natural Resources Conservation Service (NRCS). 2019. California Water Supply Outlook Report.

Null, S. E., and J. H. Viers. 2013. In bad waters: Water year classification in nonstationary climates: Water Year Classification in Nonstationary Climates. Water Resources Research 49:1137–1148.

Ottaway, E. M., P. A. Carling, A. Clarke, and N. A. Reader. 1981. Observations on the structure of brown trout, *Salmo trutta* Linnaeus, redds. Journal of Fish Biology (19):593–607.

Reiser, D., A. Olson, and K. Binkley. 1998. Sediment deposition within fry emergence traps: A confounding factor in estimating survival to emergence. North American Journal of Fisheries Management 18:713-719.

Sear, D. A., L. B. Frostick, G. Rolliston, and T. Lisle. 2008. The significance and mechanics of fine-sediment infiltration and accumulation in gravel spawning beds in Salmonid spawning habitat in rivers: physical controls, biological responses, and approaches to remediation. American Fisheries Society, Symposium 65, Bethesda, Md. pp. 121–148.

Shriver, A. J. 2015 (a). Spawning behavior and habitat selection of Chinook salmon (*Oncorhynchus tshawytscha*) within the San Joaquin River, California. SJRRP Science Symposium, Los Banos, California. June 2015.

Shriver, A. J., M. A. Meyers, J. Kirsch, and Z. Jackson. 2015 (b). Assessing spawning gravel quality within Chinook Salmon (*Oncorhynchus tshawytscha*) redds, San Joaquin River, California: Insights from the fall-run 2013 experimental population of an extirpated species. SJRRP Science Symposium, Los Banos, California. June 2015.

Shriver, A. J., M. Bandy, R. Lefler, S. Vang, M.A. Meyers, and J. Kirsch. 2016. Assessing spawning gravel quality within fall-run 2013-2015 Chinook Salmon redds, San Joaquin River, California. SJRRP Science Symposium, Fresno, California. August 2016.

Shriver, A. J. 2017. Spawning behavior and habitat selection of Chinook Salmon (*Oncorhynchus tshawytscha*) within the San Joaquin River, California. 35th Annual Salmon Restoration Conference, Davis, California. April 2017.

San Joaquin River Restoration Program (SJRRP). 2010. Fisheries Management Plan. San Joaquin River Restoration Program, Sacramento, California.

San Joaquin River Restoration Program (SJRRP). 2011. Reintroduction Strategy for Spring Run Chinook Salmon. February 2011.

San Joaquin River Restoration Program (SJRRP). 2014. Draft Seepage Management Plan. San Joaquin River Restoration Program, Sacramento, California.

San Joaquin River Restoration Program (SJRRP). 2017 Restoration Flows Guidelines Version 2.0. San Joaquin River Restoration Program, Sacramento, California.

San Joaquin River Restoration Program (SJRRP). 2018 a. SJRRP Final Flow Bench Evaluation. March 22, 2018.

San Joaquin River Restoration Program (SJRRP). 2018 b. Fisheries Framework: Spring Run and Fall-Run Chinook Salmon. San Joaquin River Restoration Program, Sacramento, California.

San Joaquin River Restoration Program (SJRRP). 2019a. Final 2019 Restoration Allocation and Default Flow Schedule. May 20, 2019.

San Joaquin River Restoration Program (SJRRP). 2019b. SJRRP Final Flow Bench Evaluation. April 5, 2019.

San Joaquin River Restoration Program (SJRRP). 2021. Fishery Management Work Group Meetings Notes. January 13, 2021.

Stark, E. J., D. T. Vidergar, C. C. Kozfkay, P. A. Kline. 2018. Egg Viability and Egg-to-Fry Survival of Captive-Reared Chinook Salmon Released to Spawn Naturally. Transactions of American Fisheries Society. Vol. 147. 13:128-138

Tappel, P. D., and T. C. Bjornn (1983), A New method of relating size of spawning gravel to salmonid embryo survival. North American Journal of Fisheries Management, 3:123-135.

Turlock Irrigation District and Modesto Irrigation District (TID/MID). 1991. Lower Tuolumne River Spawning Gravel Studies Report. Appendix 8 to Don Pedro Project Fisheries Studies Report (FERC Article 39, Project No. 2299). Vol. IV. Prepared by EA Engineering, Science, and Technology, Lafayette, California.

Traum, J. A., S. P. Phillips, G. L. Bennett, C. Zamora, and L. F. Metzger. 2014. Documentation of a groundwater flow model (SJRRPGW) for the San Joaquin River Restoration Program study area, California. U.S. Geological Survey Scientific Investigations Report 2014–5148.

Warner, G. 1991. Remember the San Joaquin. In: Lufkin, A, editor. California's salmon and steelhead. Berkeley: University of California Press. p. 61-72.

Weeber, M. A., G. R. Giannico, and S. E. Jacobs. 2010. Effects of redd superimposition by introduced kokanee on the spawning success of native bull trout. North American Journal of Fisheries Management 30.1:47-54.

Williams, G., and M. Wolman. 1984. Downstream effects of dams on alluvial rivers. U.S. Geological Survey Professional Paper 1286. 1-94.

Williams, J. G. 2006. Central Valley salmon: a perspective on Chinook and Steelhead in the Central Valley of California. San Francisco Estuary and Watershed Science 4(2).

Yoshiyama, R. M, F. W. Fisher, and P. B. Moyle. 1998. Historical abundance and decline of Chinook Salmon in the Central Valley Region of California. North American Journal of Fisheries Management 18:487-521.

Yoshiyama, R. M., E. R. Gerstung, F. W. Fisher, and P. B. Moyle. 2000. Chinook salmon in California's Central Valley: an assessment. Fisheries 25(2):6–20.

Yoshiyama, R. M, E. R. Gerstung, F. W. Fisher, and P. B. Moyle. 2001. Historical and present distribution of Chinook salmon in the Central Valley drainage of California. Pages 71–177 in R. L. Brown, editor. Contributions to the biology of Central Valley salmonids. Volume 1. California Department of Fish and Game Fish Bulletin 179.

Zhou, S. 2002. Size-dependent recovery of Chinook Salmon in carcass surveys. Transactions of the American Fisheries Society 131:1194–1202.

Zuur, A. F., E. N. Ieno, N. J. Walker, A. A. Saveliev, and G. M. Smith. 2009. Mixed effects models and extensions in ecology with R. Springer.

Personal Communications

P. Adelizi. 2020. Personal Communication between Paul Adelizi of the California Department of Fish and Wildlife and Austin Demarest of U.S. Fish and Wildlife Service regarding 2018 to 2019 fecundity estimates for the Salmon Conservation Research Facility broodstock and Feather River Fish Hatchery returning spring-run Chinook Salmon. October 5, 2020.

Z. Sutphin, 2021. Personal Communication between Zak Sutphin of the U.S. Bureau of Reclamation and Austin Demarest of the U.S. Fish and Wildlife Service regarding rotary screw trap capture totals via email. May 20, 2021.

Tables

Table 1. Spring-run Chinook Salmon redd characteristics observed within Reach 1 of the San Joaquin River Restoration Area from 2016 to 2019.

	2016			2017			2018			2019		
Variable	Mean	SD	Range	Mean	SD	Range	Mean	SD	Range	Mean	SD	Range
Redd area (m^2)	3.1	1.2	1.7-4.1	5.0	2.5	1.8-9.8	3.3	1.9	0.9-9.7	9.1	5.5	1.0-27.5
Tailspill area (m^2)	2.4	1.0	1.4-3.3	2.8	1.3	1.1-5.0	1.8	0.9	0.5-3.9	5.4	3.6	0.6-19.5
Pit area (m^2)	0.7	0.3	0.4-0.8	2.2	1.4	0.6-5.2	1.4	1.1	0.3-5.8	3.7	2.4	0.4-13.4
Pit excavation Depth (m)	0.1	0.1	0.0-0.1	0.1	0.0	0.0-0.2	0.1	0.1	0.1-1.3	0.1	0.1	0.0-1.3
Depth upstream pre-redd (m)	0.4	0.1	0.3-0.5	0.5	0.2	0.3-0.8	0.5	0.3	0.2-1.1	0.5	0.2	0.1-1.2
Pre-redd velocity (m/s^2)	0.7	0.2	0.5-0.9	0.6	0.2	0.3-0.9	0.7	0.3	0.2-1.5	0.6	0.3	0.00-1.5

Table 2. Summary of spring-run Chinook Salmon redd spawn site habitat classification (riffles, runs, glides, and pools) in the San Joaquin River Restoration Area from 2016 to 2019.

	2016	2017	2018	2019
Redd total	3	16	42	209
Riffles	1	12.50%	42.86%	38.76%
Runs	-	62.50%	45.24%	36.36%
Glides	-	-	-	22.97%
Pools	-	-	-	1.91%
Undocumented	-	25%	11.90%	-

Table 3. Summary of count, sex, and spawn status for ancillary excess broodstock, translocated, and volitionally returned adult spring-run Chinook Salmon carcasses recovered in Reach 1 of the San Joaquin River Restoration Area in 2019. Two volitional return carcasses have been excluded from this table due the condition of the carcasses being too degraded to determine gender.

	Broodstock		Translocated Hatchery Return		Volitional Hatchery Return	
	Female	Male	Female	Male	Female	Male
Fish released	37	77	12	6	-	-
Carcasses recovered	9	7	2	1	104	43
% Recovery	24%	9%	17%	17%	-	-
Mean fork length mm (SD)	589 (129)	544 (86)	700 (57)	758 (-)	704 (40)	790 (64)
% Unspawned	11%	-	50%	-	6%	-
% Spawned	89%	-	50%	-	92%	-

Table 4. Summary of coded wire tag (CWT) codes, hatchery origin, brood year, and sex of translocated, volitionally returned, and broodstock spring-run Chinook Salmon carcasses recovered in 2019 in Reach 1 of the San Joaquin River Restoration Area. All carcasses recovered originated from the Feather River Fish Hatchery (FRFH) or Salmon Conservation and Research Facility (SCARF), all of which were from released by San Joaquin River Restoration Program.

			Translocated Hatchery Return		Volitional Hatchery Return			Broodstock	
CWT Code	Hatchery Origin	Brood Year	Male	Female	Male	Female	Unknown	Male	Female
61406	FRFH	2016	1	-	9	44	1	-	-
61423	SCARF	2016	-	2	19	38	-	-	-
61424	SCARF	2016	-	-	9	14	-	-	-
60514	FRFH	2015	-	-	-	-	-	4	5
61420	SCARF	2016	-	-	-	-	-	1	-
61421	SCARF	2016	-	-	-	-	-	2	2
No CWT		-	-	-	6	7	1	-	1
CWT lost		-	-	-	-	1	-	-	1

Table 5. Fry emergence start and end accumulated thermal unit (ATU), emergence duration, count, incidental mortality, size, and excavated egg count during 2018 and 2019 within Reach 1 of the San Joaquin River Restoration Area. Data are derived from point data measured during emergence trap checks. The rkm is the river kilometer location of the trapped redd.

Year	Redd #	Location (rkm)	Start (ATU)	End (ATU)	Days of Emergence	Fry Count	Mortality Count	*Fry Size (mm)*		Eggs Found
								Mean (SD)	Range	
2018	NR02SR18[a]	420	0	0	0	0	0	---	---	0
2018	NR10SR18	421	954	1071	9	5	1	32 (2.5)	28-34	465
2018	NR17SR18[a]	429	0	0	0	0	0	---	---	0
2018	NR21SR18[a]	412	875	1025	12	6	3	32 (1.1)	31-33	0
2018	NR25SR18[b]	424	1053	1053	1	1	0	0	---	159
2018	NR27SR18	420	785	1229	37	6	2	32 (2.7)	28-35	131
2018	NR28SR18	419	638	973	25	18	8	33 (1)	31-35	156
2018	NR33SR18[a]	418	998	1010	1	129	19	36 (1.2)	34-39	0
2018	NR40SR18[d]	416	0	0	0	0	0	---	---	---
2018	NR42SR18[d]	412	0	0	0	0	0	---	---	---
2019	NR03SR19[b]	429	809	1398	46	1432	354	33 (2.0)	28-48	4
2019	NR12SR19[b,c]	418	1177	1177	1	1	1	34 (0)	34	---
2019	NR30SR19[a]	422	631	978	20	63	12	27 (2.4)	22-34	0
2019	NR43SR19[b]	416	631	1238	38	1725	16	33 (1.6)	18-38	37
2019	NR57SR19[a]	429	735	1540	73	1097	7	36 (5.5)	29-56	0
2019	NR125SR19	426	670	1377	60	758	40	32 (1.9)	26-38	1
2019	NR128SR19[b,c]	423	699	972	20	283	22	33 (0.7)	31-35	---
2019	NR159SR19	429	902	>1630*	71	416	5	40 (6.8)	32-56	1
2019	NR189SR19	429	1090	1090	1	1	1	38 (0)	38	307
2019	NR190SR19[a]	429	685	>1413*	70	1379	7	32 (2.0)	26-56	0
2019	NR196SR19	429	684	>1399*	70	774	204	33 (1.5)	29-44	48
2019	NR204SR19[a]	428	689	>1602*	81	495	6	31 (2.7)	24-50	0

[a] Indicates no eggs were found during excavation.
[b] Indicates that the cod end jar came off during sampling.
[c] Indicates that the redd was not excavated due to water depth or velocity.
[d] Indicates the redd was not excavated due to being removed early.
*Indicates the redd was still producing fry when the trap was removed.

Table 6. Predictor variables, number of parameters, Akaike Information Criterion with correction for finite sample sizes (AICc), difference in AICc from the best model (ΔAICc), and Akaike weights (W_i) for the set of candidate generalized linear models predicting the number of salmon emerging from redds monitored within the San Joaquin River Restoration Area in 2018 and 2019. Note that a data point found to be an influential outlier was removed from the data set. Values of W_i below 0.001 are listed as 0.00.

Predictor Variables	Number of Parameters	AIC_c	ΔAIC_c	W_i
Year	3	186.16	0	0.51
Year + Pit depth	4	188.06	1.90	0.20
Year + Velocity above	4	189.36	3.21	0.10
Year + 10-day max temperature	4	189.60	3.44	0.09
Year + Egg pocket height	4	189.65	3.49	0.09
Year + 10-day max temp + Velocity above	5	193.48	7.33	0.01
Dissolved oxygen	5	199.98	13.82	0.00
Velocity above + Dissolved oxygen	7	205.85	19.68	0.00
Mean temperature	3	206.74	20.58	0.00
Dissolved oxygen + 10-day max temp	7	207.31	21.15	0.00
Percent sand	3	209.58	23.42	0.00
Pit depth	3	211.16	25.01	0.00
Velocity above	3	211.82	25.66	0.00
Mean flow	5	212.44	26.28	0.00
Egg pocket height	3	212.63	26.47	0.00
Max temperature	3	212.88	26.72	0.00
10-day max temp + Mean flow	7	214.89	28.73	0.00
Velocity above + Percent sand	7	215.61	29.45	0.00
Tailspill depth	5	217.72	31.56	0.00
Tailspill depth + Mean flow	7	217.92	31.77	0.00
Mean flow + Velocity above	7	222.05	35.89	0.00

Table 7. Predictor variables, number of parameters, Akaike Information Criterion with correction for finite sample sizes (AICc), difference in AICc from the best model (ΔAICc), and Akaike weights (W_i) for the set of candidate generalized linear models predicting the number of salmon emerging from redds monitored within the San Joaquin River Restoration Area in 2018 and 2019.

Predictor Variables	Number of Parameters	AIC_c	ΔAIC_c	W_i
Year + Pit depth	4	209.44	0	0.37
Year + Velocity above	4	210.13	0.69	0.26
Year	3	210.87	1.44	0.18
Dissolved oxygen	5	213.14	3.71	0.06
Year + Egg pocket height	4	213.64	4.20	0.05
Year + 10-day max temp + Velocity above	5	213.93	4.50	0.04
Year + 10-day max temp	4	214.24	4.81	0.03
Velocity above + Dissolved oxygen	7	219.35	9.91	0.00
Mean temp	3	220.05	10.61	0.00
Dissolved oxygen + 10-day max temp	7	221.85	12.42	0.00
Percent sand	3	222.69	13.26	0.00
Velocity above	3	225.64	16.21	0.00
Egg pocket height	3	226.12	16.68	0.00
Max temp	3	226.49	17.06	0.00
Mean flow	5	226.57	17.14	0.00
Velocity above + Percent sand	7	227.78	18.35	0.00
Tailspill depth	5	231.68	21.64	0.00
Pit depth	5	232.21	22.78	0.00
10-day max temp + Mean flow	7	232.39	22.95	0.00
Tailspill depth + Mean flow	7	232.99	23.55	0.00
Mean flow + Velocity above	7	235.41	25.97	0.00

Table 8. Results from generalized linear models used to assess the relationship between emergence counts and standardized environmental and redd characteristic factors within the San Joaquin River Restoration Area in 2019.

Response Variable	Parameter	Estimate	SE	*df*	Z Value	*p* Value
Emergence	Intercept	5.14	1.45	14	4.407	1.05 E-05
	Year 2019	175.43	1.61		10.918	< 2 E-16

Table 9. Mean environmental characteristics for each emergence trapped redd in the San Joaquin River Restoration Area in 2018 and 2019. Data are derived from point data measured during emergence trap checks.

Redd #	Dissolved Oxygen (mg/L)	Turbidity (NTU)	Temperature (°C)	Depth (m) Above trap	Depth (m) Below Trap	Velocity (m/s) Above Trap	Velocity (m/s) Below Trap
NR02SR18	9.28	2.17	12.15	0.31	0.29	0.56	0.66
NR10SR18	9.19	2.25	11.91	0.44	0.32	0.36	0.81
NR17SR18	8.98	5.46	12.30	0.39	0.41	0.45	0.53
NR21SR18	9.97	2.52	12.03	0.45	0.37	0.77	1.02
NR25SR18	9.55	2.14	12.02	0.48	0.40	0.61	0.95
NR27SR18	9.34	3.00	11.81	0.60	0.59	0.59	0.81
NR28SR18	9.40	2.54	11.84	0.54	0.35	0.43	0.75
NR33SR18	9.80	2.09	12.07	0.79	0.61	0.75	1.07
NR40SR18	10.00	2.19	11.60	0.63	0.64	0.83	1.05
NR42SR18	10.64	1.96	10.94	0.44	0.40	0.94	1.18
NR03SR19	10.51	4.90	12.39	0.55	0.35	0.73	1.05
NR12SR19	10.99	2.02	11.58	0.60	0.52	1.01	1.32
NR30SR19	10.80	2.28	11.71	0.59	0.62	0.51	0.57
NR43SR19	10.88	2.14	11.45	0.67	0.58	0.78	0.97
NR57SR19	10.42	2.25	11.73	0.51	0.49	0.40	0.57
NR125SR19	11.31	2.48	11.90	0.66	0.54	0.76	0.82
NR128SR19	11.13	2.31	11.32	0.66	0.57	0.87	1.01
NR159SR19	10.52	2.62	11.65	0.37	0.38	0.44	0.39
NR189SR19	10.67	2.47	11.14	0.45	0.26	0.63	0.90
NR190SR19	10.54	2.50	11.18	0.52	0.42	0.69	0.74
NR196SR19	10.62	2.48	10.98	0.31	0.26	0.65	0.91
NR204SR19	10.68	2.24	11.99	0.54	0.54	0.55	0.59

Table 10. Annual mean environmental characteristics measured during the 2018 to 2019 emergence trap checks in the San Joaquin River Restoration Area. Dissolved oxygen (mg/L) and water temperature (°C) were measured at the substrate surface, turbidity (NTU) measured just below the water surface, top and bottom depth, and velocity (m/s) measured 60 percent below the water surface, above and below emergence traps in 2018 and 2019 with associated standard deviation (SD). Data are derived from point data measured during emergence trap checks.

Year	Mean (SD)	DO (mg/L)	Turbidity (NTU)	Temperature (°C)	Top Depth (m)	Bottom Depth (m)	Velocity Above (m/s)	Velocity Below (m/s)
2018	Mean	9.62	2.63	11.87	0.51	0.44	0.63	0.88
	(SD)	0.49	1.04	0.38	0.14	0.13	0.19	0.20
2019	Mean	10.76	2.56	11.58	0.53	0.46	0.67	0.82
	(SD)	0.27	0.76	0.40	0.11	0.12	0.18	0.26

Table 11. Annual mean adult spring-run Chinook Salmon fecundity and egg-to-fry survival estimates. Percent egg-to-fry survival was calculated using the estimated fecundity of broodstock at Salmon Conservation and Research Facility (SCARF) or natural returns at Feather River Fish Hatchery (FRFH).

Year	Fecundity SCARF Broodstock	Fecundity FRFH Hatchery Returns	Number of Emergence Traps	Mean Fry Emergence	Egg-to-Fry Survival SCARF Broodstock (%)	Egg-to-Fry Survival FRFH Hatchery Returns (%)
2018	3,068	4,558	6	27.5	0.90	0.60
2019	3,247	5,523	12	702	21.62	12.71

Figures

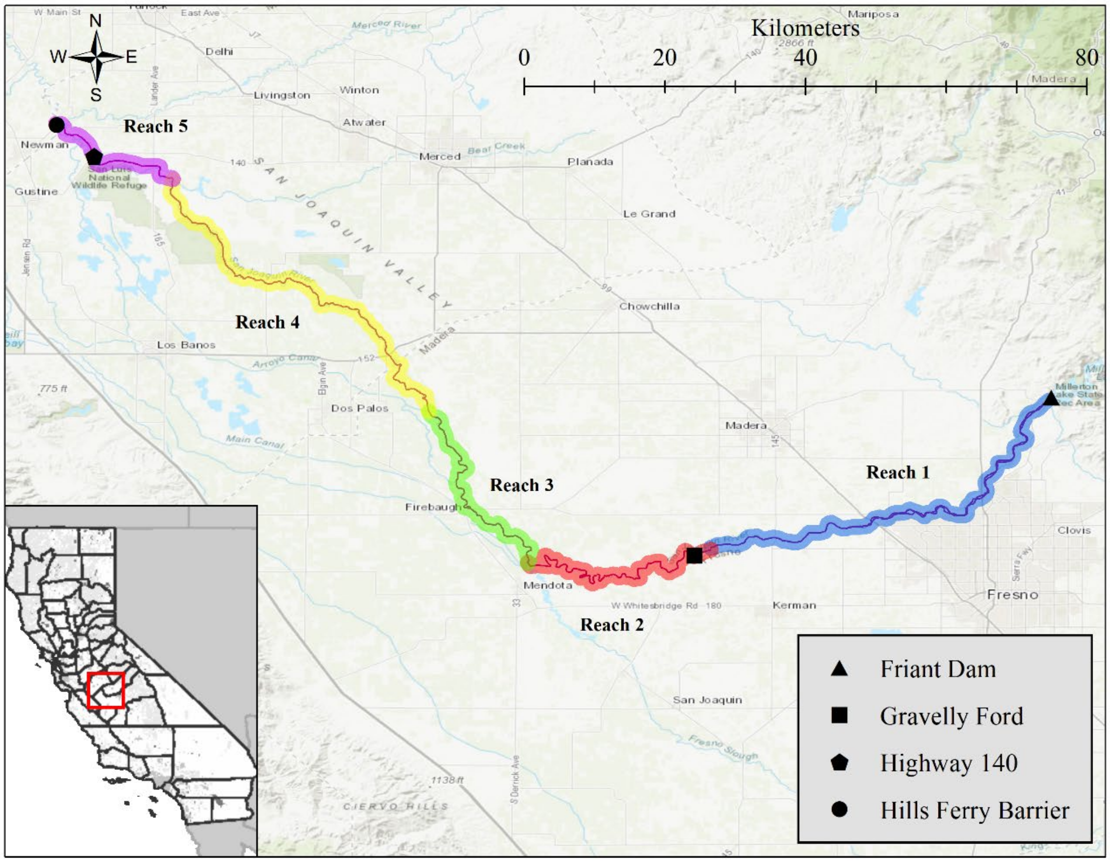

Figure 1.The San Joaquin River Restoration Area within the San Joaquin River, California. The San Joaquin River Restoration Area is stratified into five reaches which are delineated using labels and unique colored lines. The five reaches of the Restoration Area span from Friant Dam (rkm 431) to the confluence of the San Joaquin River with the Merced River (rkm 190).

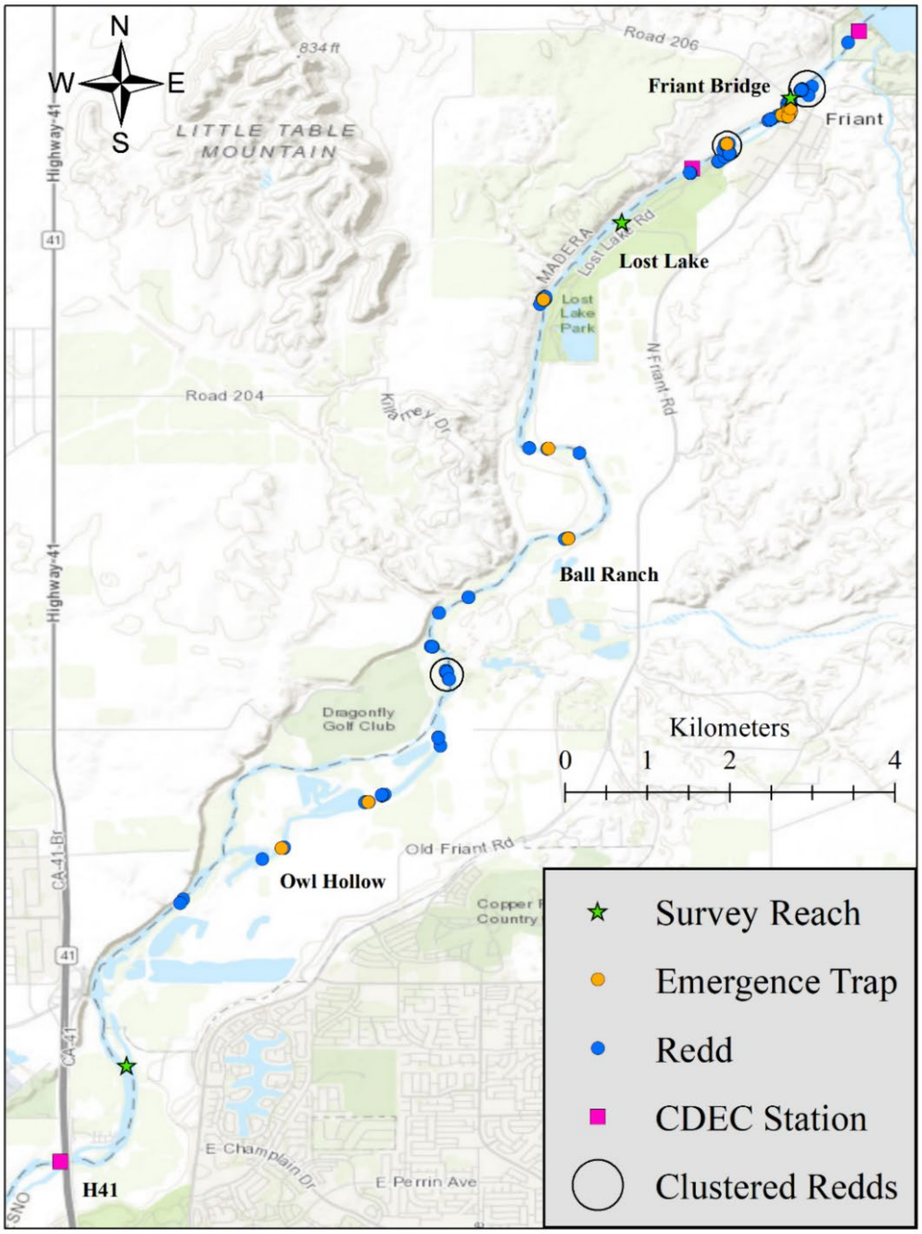

Figure 2. The locations of spring-run Chinook Salmon redds, (September 1 to November 1, 2019) areas with clustered redds, and the twelve redds selected for emergence traps (October 31, 2019 to February 13, 2020) in Reach 1 of the San Joaquin River Restoration Area. The survey reaches for redd monitoring and carcass survey are labeled with green stars, and California Data Exchange Center (CDEC, http://cdec.water.ca.gov) temperature gages are labeled with pink squares. Survey reaches were broken into 3 days: Friant Dam (rkm 431) to Lost Lake (rkm 426), Lost Lake (rkm 426) to Fresno Sportsmen’s Club (rkm 414), and Sportsmen's Club (rkm 414) to Milburn Ecological Unit (rkm 398; not pictured).

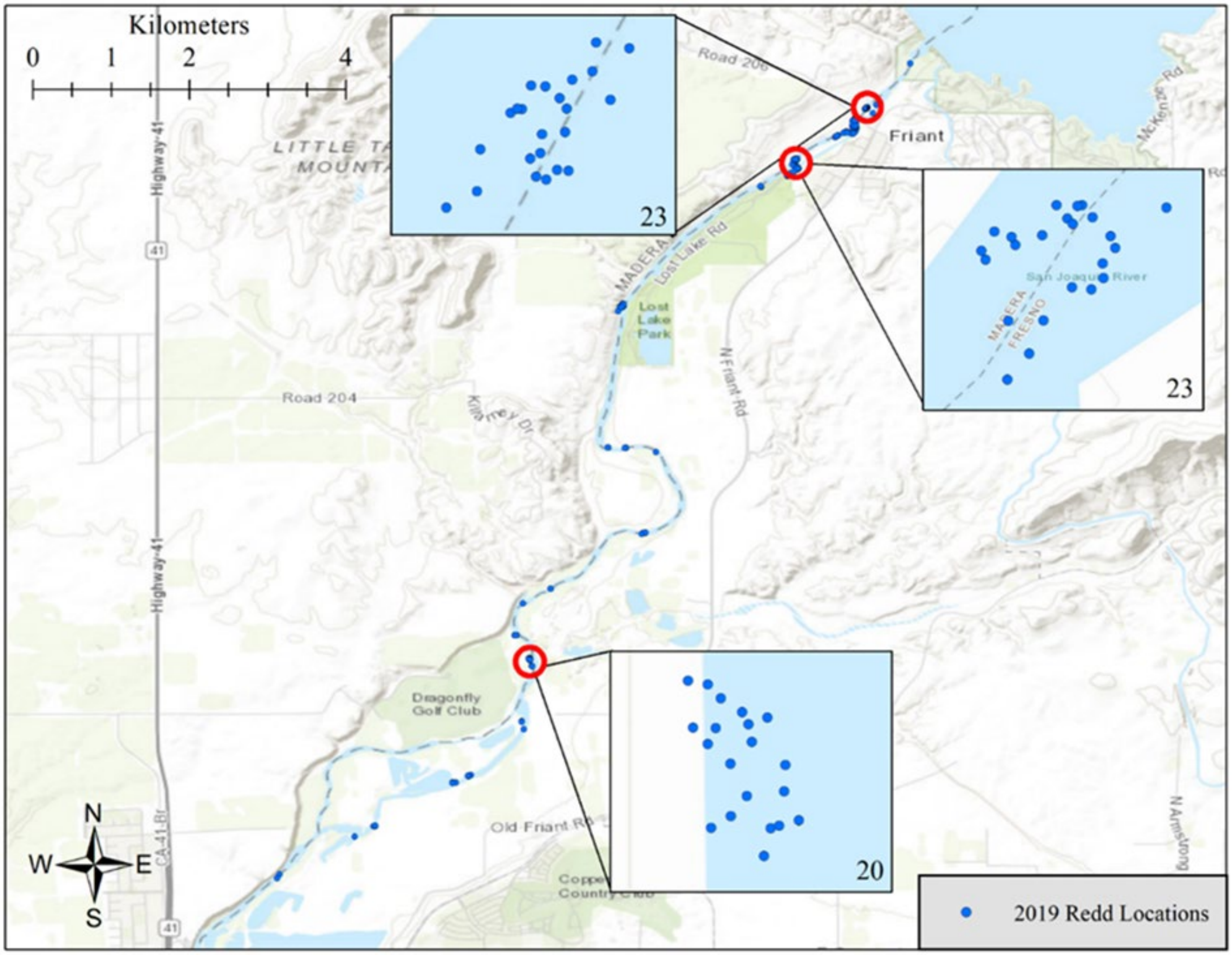

Figure 3. Spring-run Chinook Salmon redd locations identified in the San Joaquin River Restoration Area during the 2019 spawning season. The inset map indicates the individual redds within clustered areas.

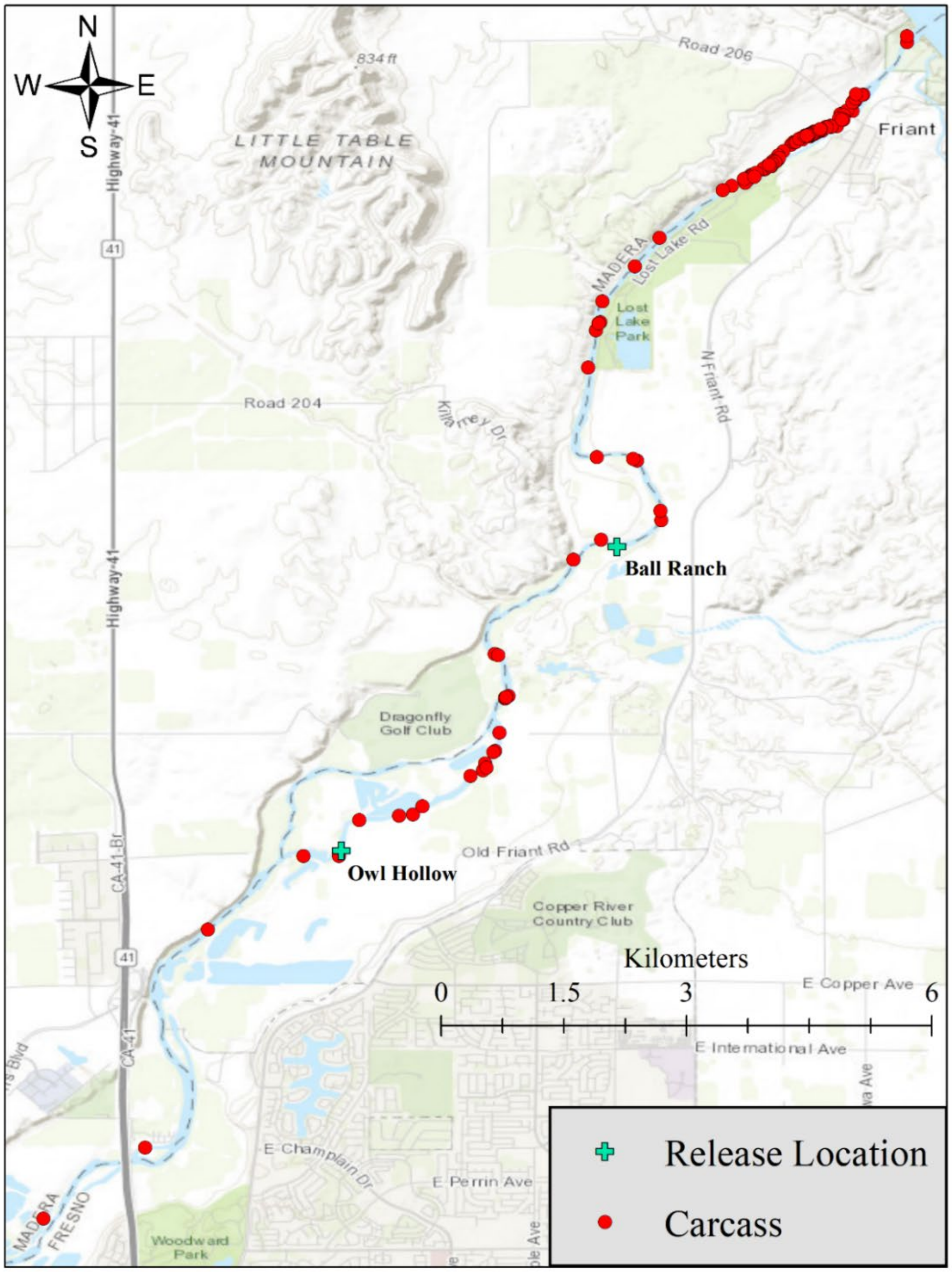

Figure 4. The locations of recovered adult spring-run Chinook Salmon carcasses (August 29 to November 5, 2019) and release sites for the adult spring-run Chinook Salmon broodstock (May to August 2019) within the San Joaquin River Restoration Area.

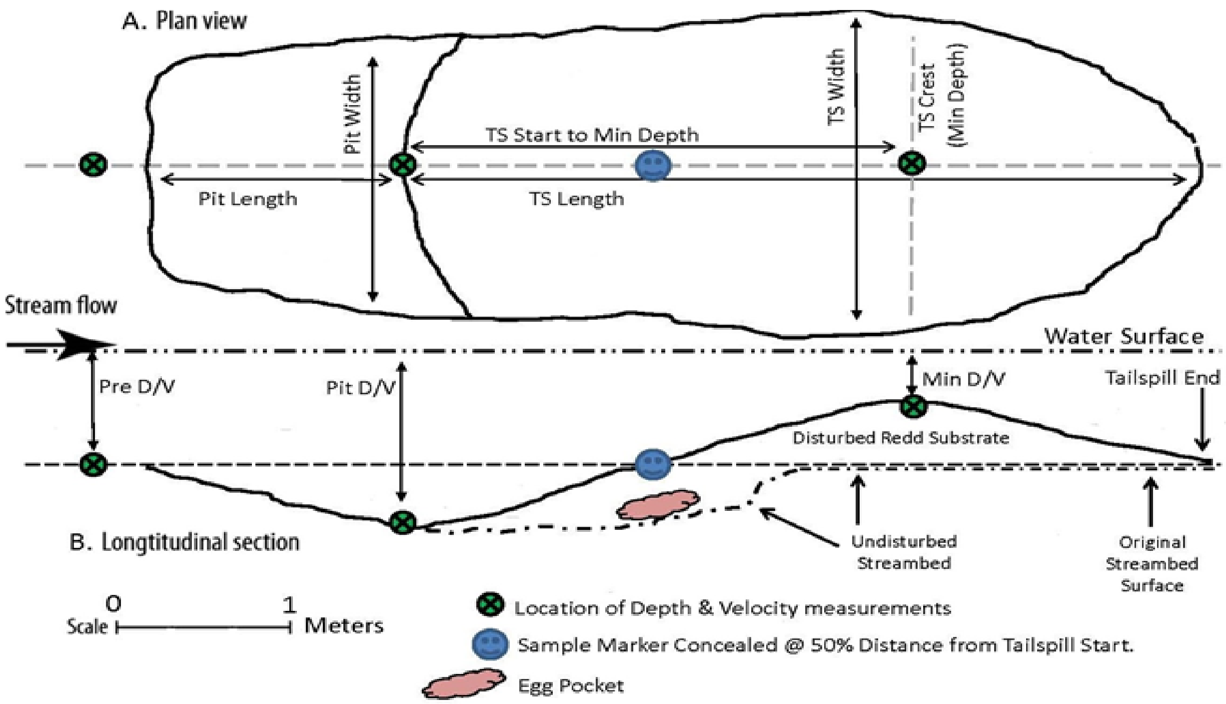

Figure 5. Plan view (A), longitudinal view (B), and corresponding measurements and features of a typical Chinook Salmon redd.

Figure 6. A recovered broodstock spring-run Chinook Salmon carcass. Measuring tape and identification tag indicating recorded data.

Figure 7. An emergence trap installed during 2019. The red arrow indicates flow direction.

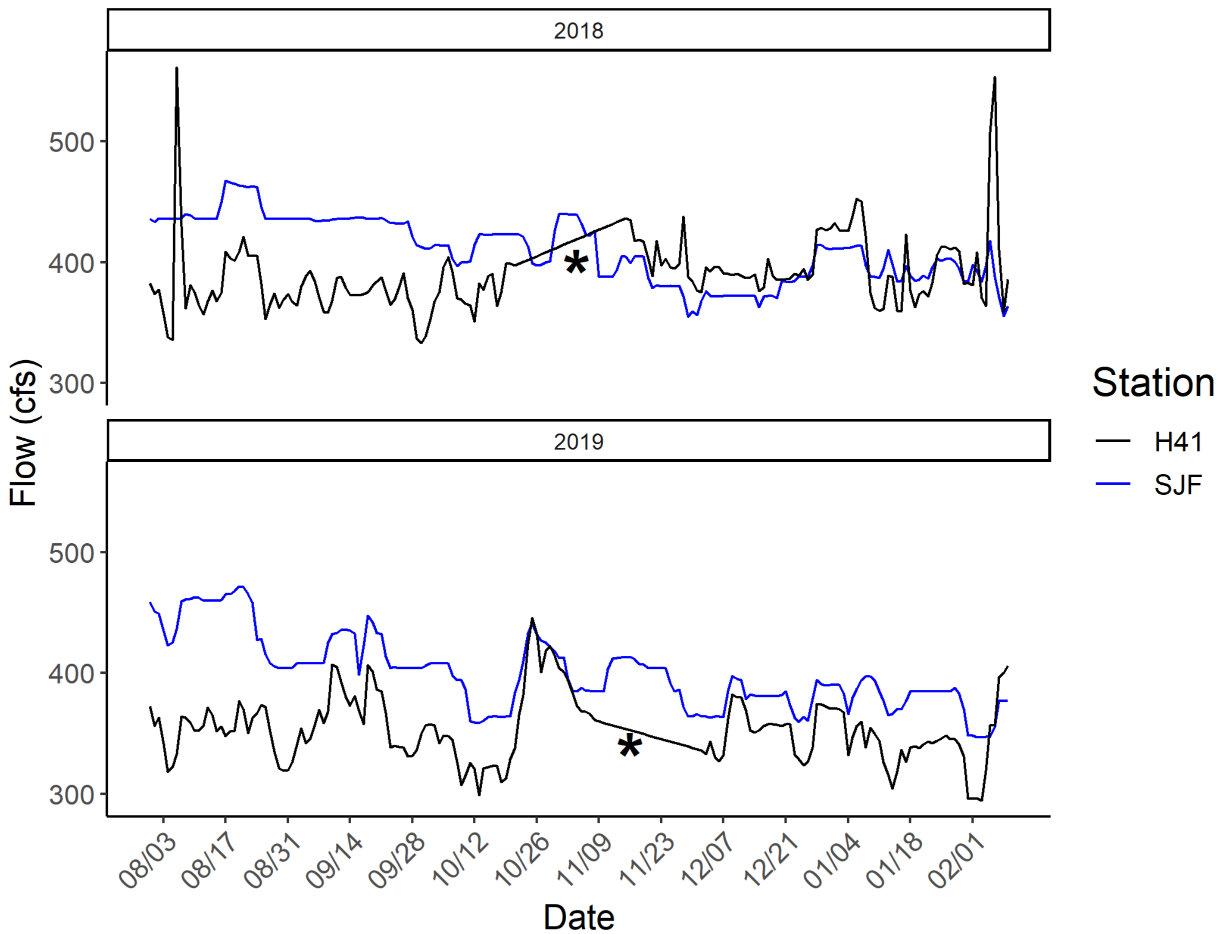

Figure 8. Mean daily river flow (cfs) recorded in the San Joaquin River below Friant Dam (rkm 430, SJF) and Highway 41 (rkm 410, H41) from August 2018 to February 2019 and August 2019 to February 2020. Flow data were obtained from the California Data Exchange Center (CDEC, http://cdec.water.ca.gov). The asterisk (*) indicates missing H41 gage data. See text for more information.

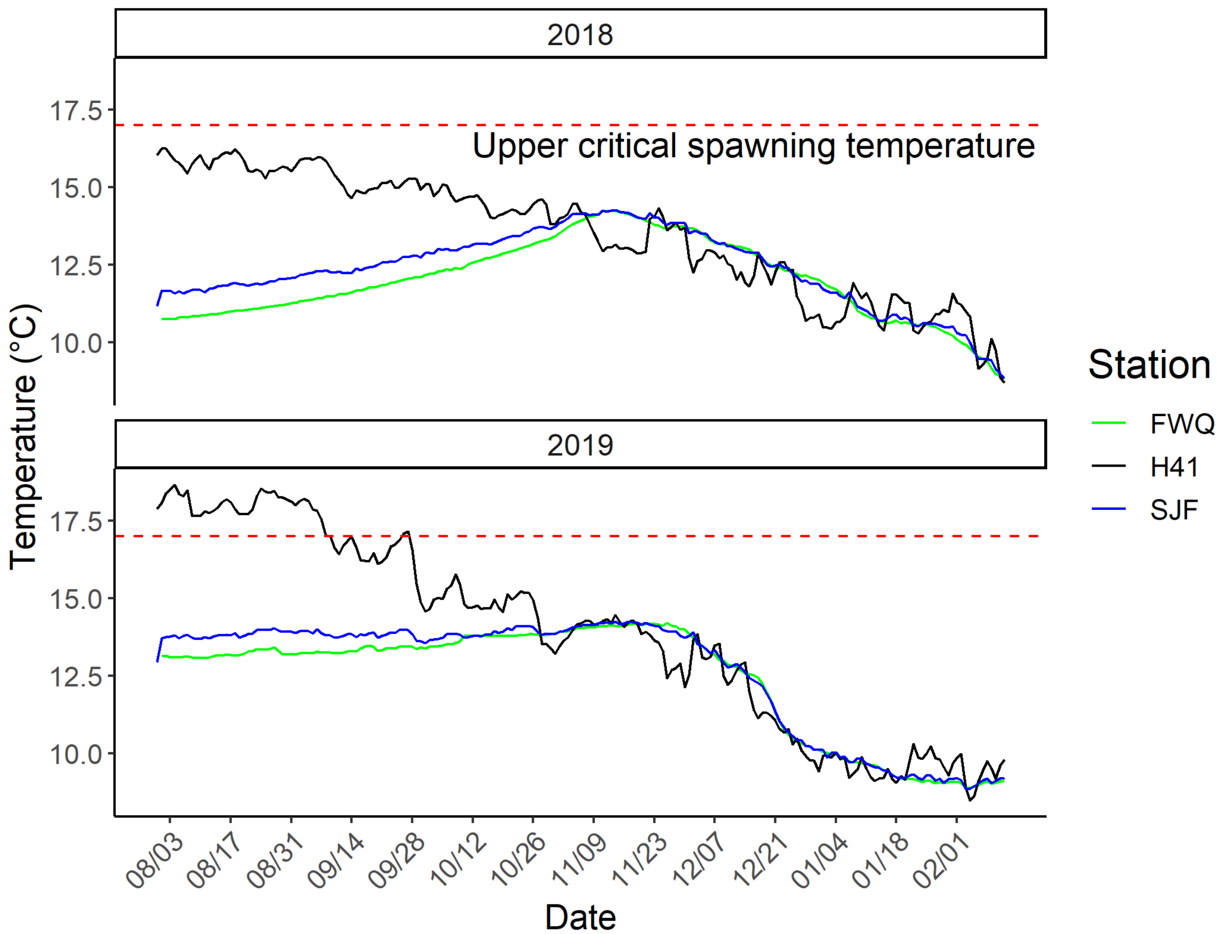

Figure 9. Mean daily water temperature (°C) recorded in the San Joaquin River downstream of Friant Dam (rkm 428 and rkm 430; San Joaquin River below Friant [SJF] and Friant Water Quality [FWQ]) and below Highway 41 (rkm 410; H41) from August 2018 to February 2019 and August 2019 to February 2020. Temperature data were obtained from the California Data Exchange Center (CDEC, http://cdec.water.ca.gov). The upper critical temperature threshold for Chinook Salmon spawning is indicated by the red dashed line at 17 °C (SJRRP 2010). See text for more information.

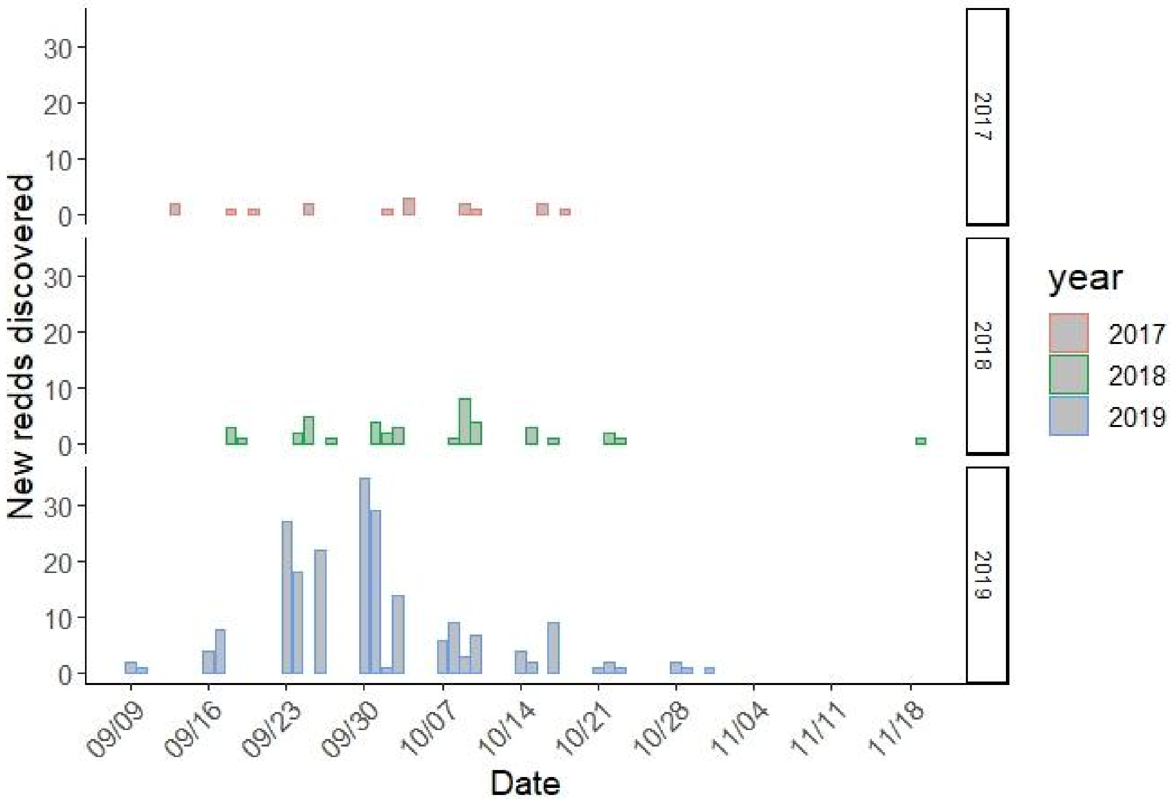

Figure 10. Summary of the total number of spring-run Chinook Salmon redds detected each survey day in Reach 1 of the San Joaquin River Restoration Area from 2017 to 2019.

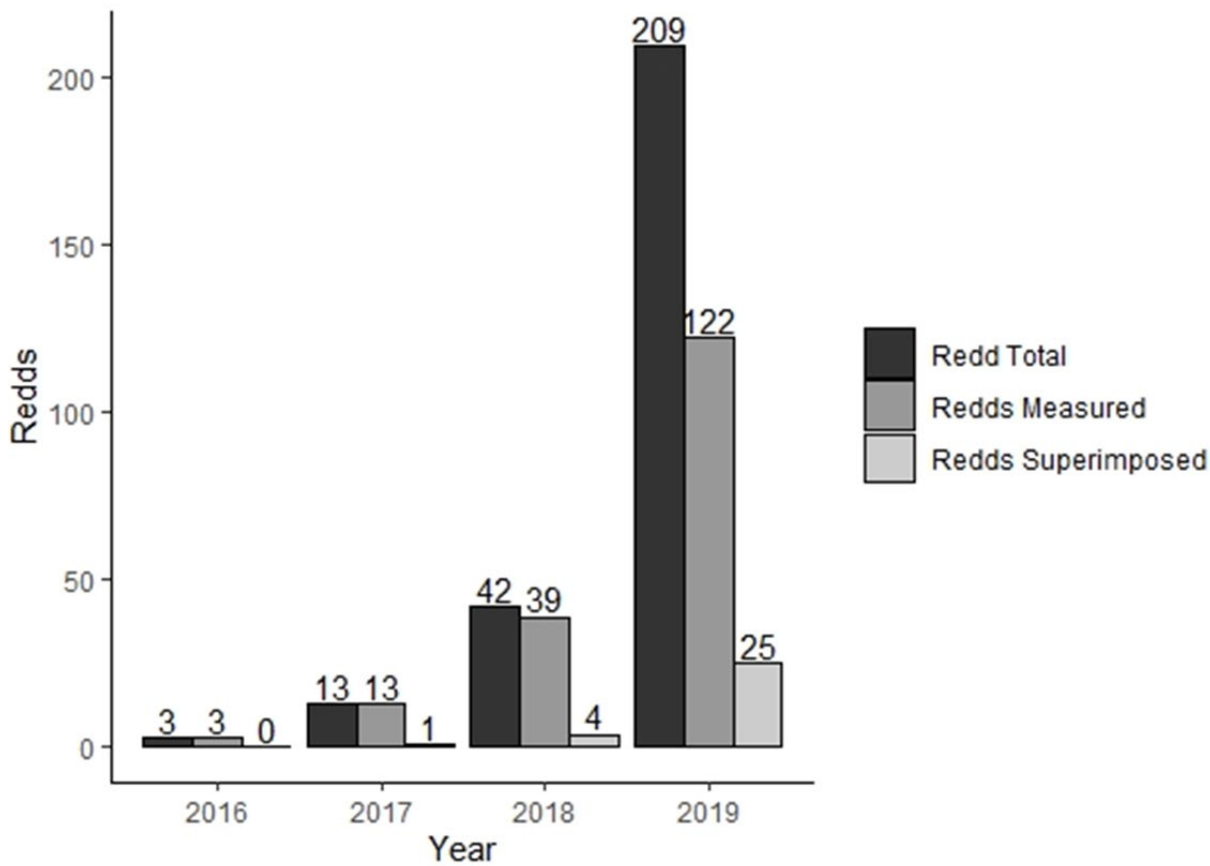

Figure 11. Summary of the total number of spring-run Chinook Salmon redds detected, measured, and superimposed upon from 2016 to 2019.

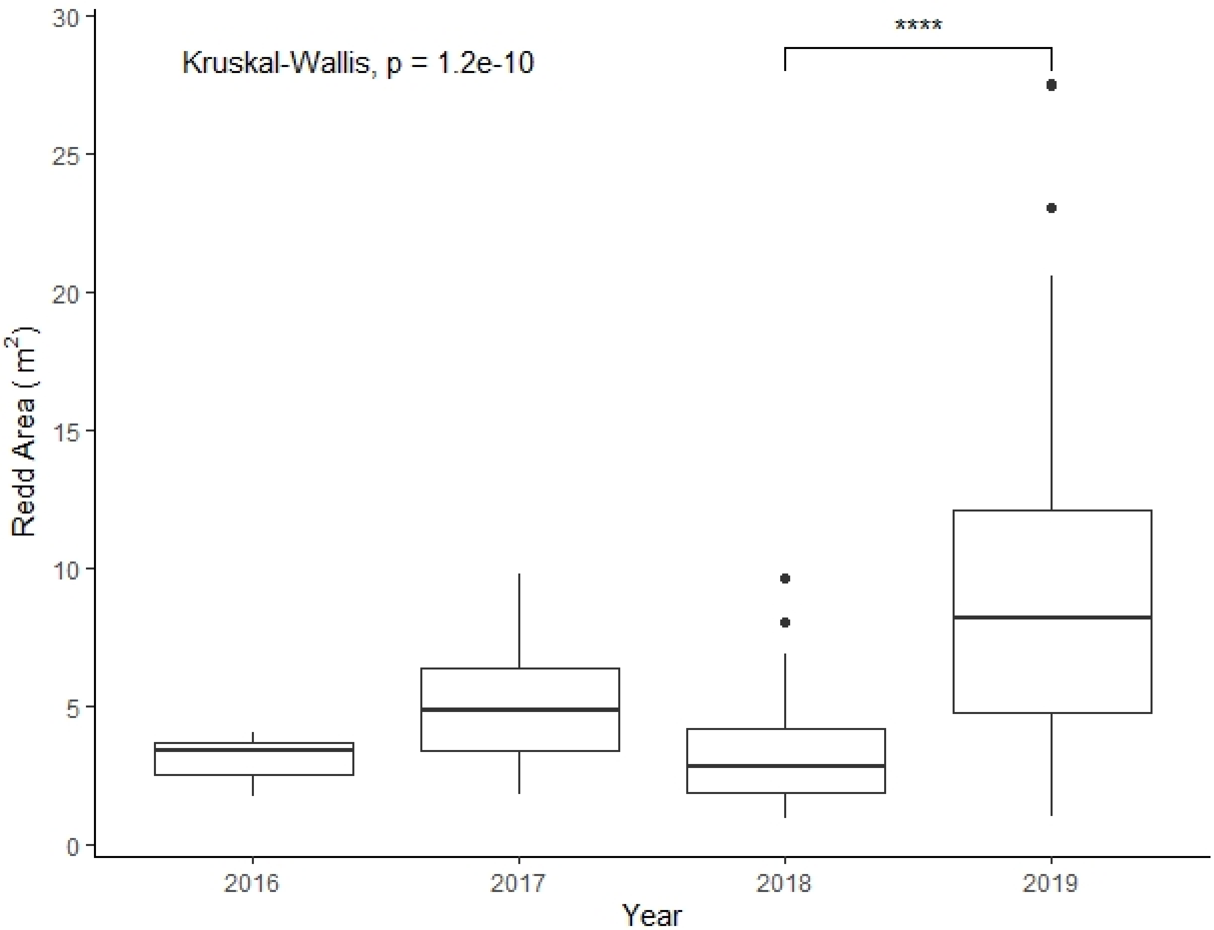

Figure 12. Boxplot of redd area (m2) from 2016 to 2019. The whiskers extend to the minimum and maximum values, the horizontal dotted lines represent the maximum (9.8 m^2) and minimum (0.94 m^2) area of redds documented from 2016 to 2018, and the dots above represent outliers. The Kruskal-Wallis test indicated a difference in redd size among years (p = 1.2 E-10), related only to a significant difference between years 2018 and 2019, as indicated by *** ($p < 0.0001$).

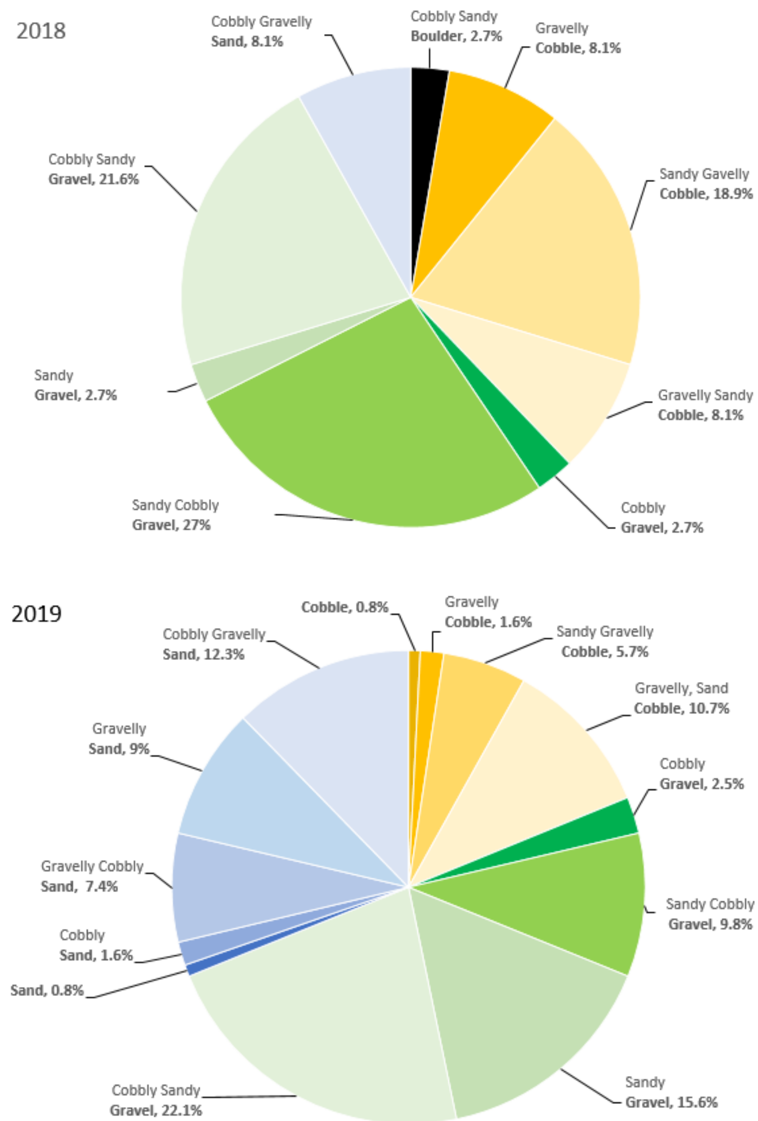

Figure 13. Percent of redds within each facies category for 2018 (n = 37) and 2019 (n = 122). Redds from 2017 were excluded due to a small sample size (n = 13).

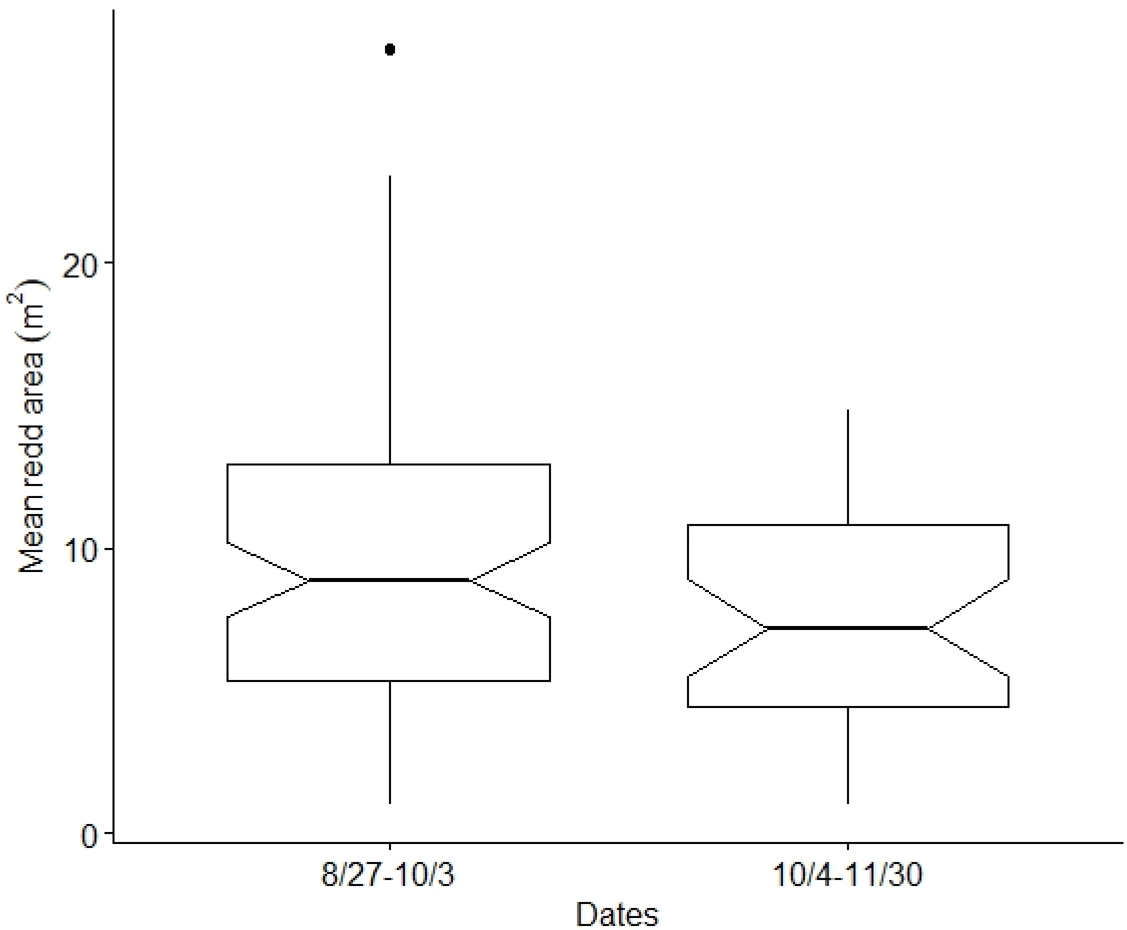

Figure 14. Comparison between mean redd area for redds documented while broodstock were acoustically detected near Friant Dam in the San Joaquin River to redds that were documented after detections ceased. The mean redd area from redds identified 8/27 to 10/3 in 2019 was 9.61 m^2 (SD 5.83), whereas the mean redd area from redds identified 10/4 to 11/30 in 2019 was 7.28 m^2 (SD 4.02). The boxes represent the 1st and 3rd quartiles (25th and 75th percentiles) of the data range, the horizontal line represents the median, the whiskers extend to the minimum and maximum values, the notches represent the 95 percent confidence intervals of the median, and the dot above group 1 is an outlier.

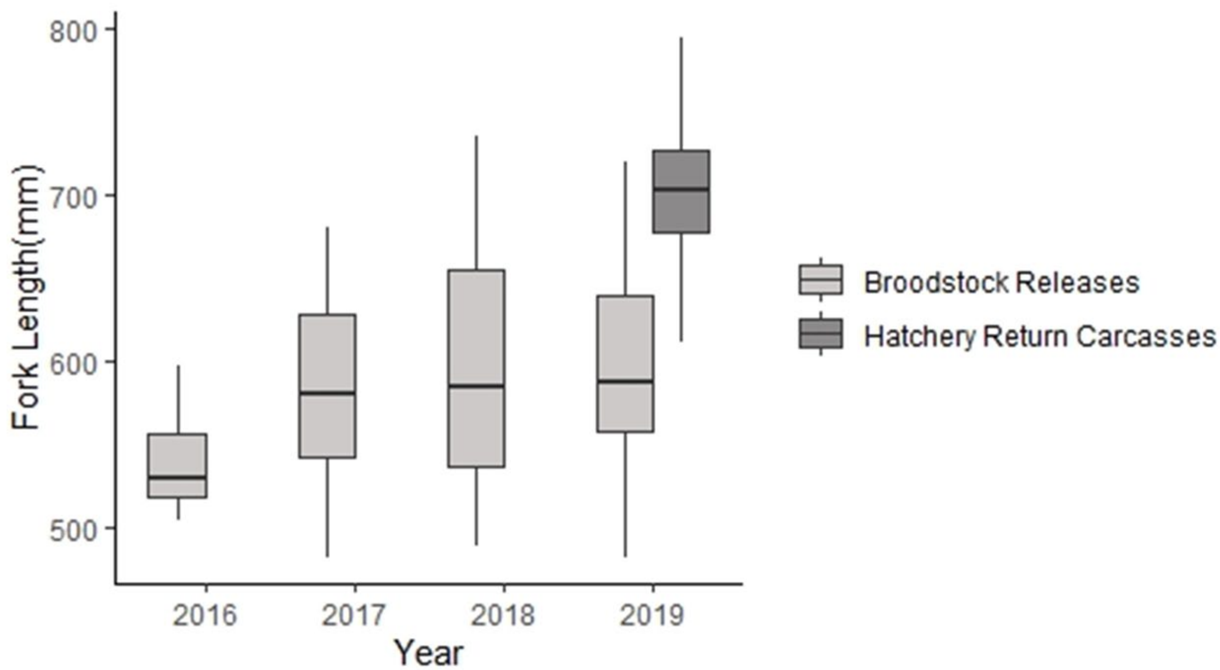

Figure 15. Summary of the distribution by fork length (mm) of broodstock upon release and both translocated hatchery return and volitional hatchery return carcasses recovered from 2016 to 2019. The boxes represent the 1st and 3rd quartiles (25th and 75th percentiles) of the data range, the horizontal line represents the median, and the whiskers extend to the minimum and maximum values.

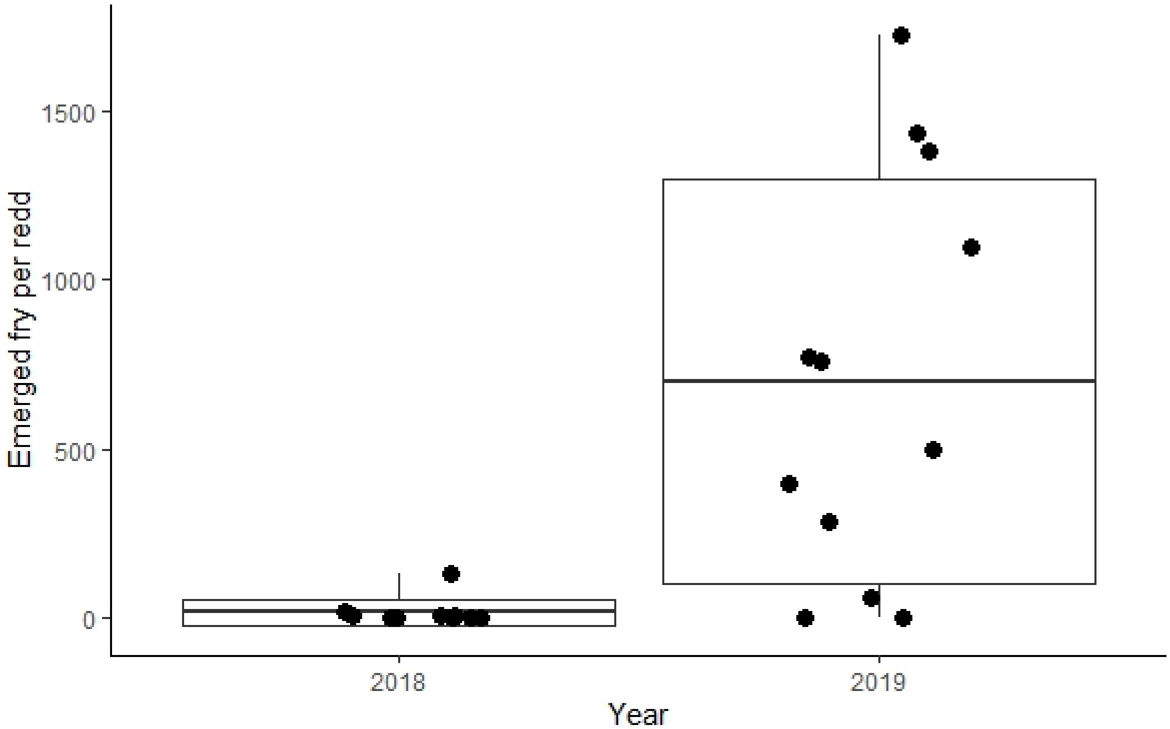

Figure 16. Comparison of the total number of emerged fry from each spring-run Chinook Salmon redd capped by an emergence trap between the 2018 (October 30, 2018 to February 8, 2019) and 2019 (October 31, 2019 to February 13, 2020) emergence trap sampling seasons near Friant Dam in the San Joaquin River. Three of the 22 total redds were excluded due to being test redds or redds of undetermined spawning status. Box plots show the mean (middle horizontal line) plus or minus the standard deviation, along with whiskers that extend to the minimum and maximum values. Points overlaying the box plots are data from individual redds.

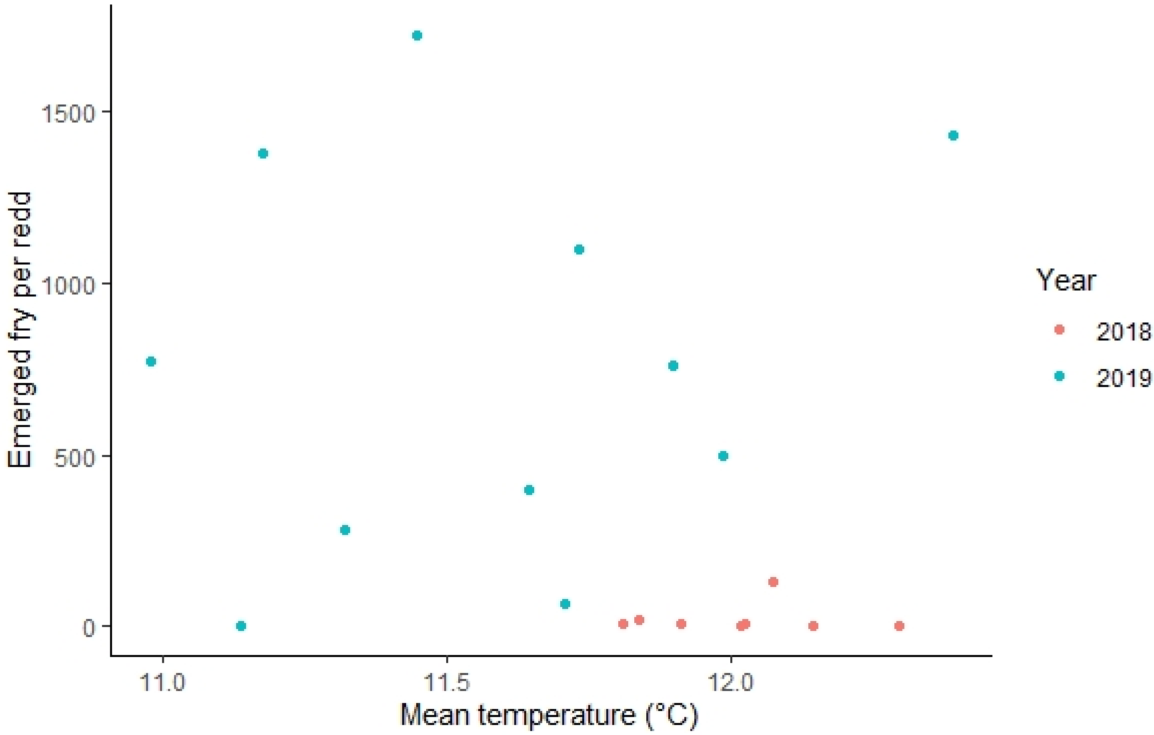

Figure 17. Total fry emergence per redd and mean temperature (°C) based on periodic field checks at spring-run Chinook Salmon redds in the San Joaquin River Restoration Area in 2018 and 2019.

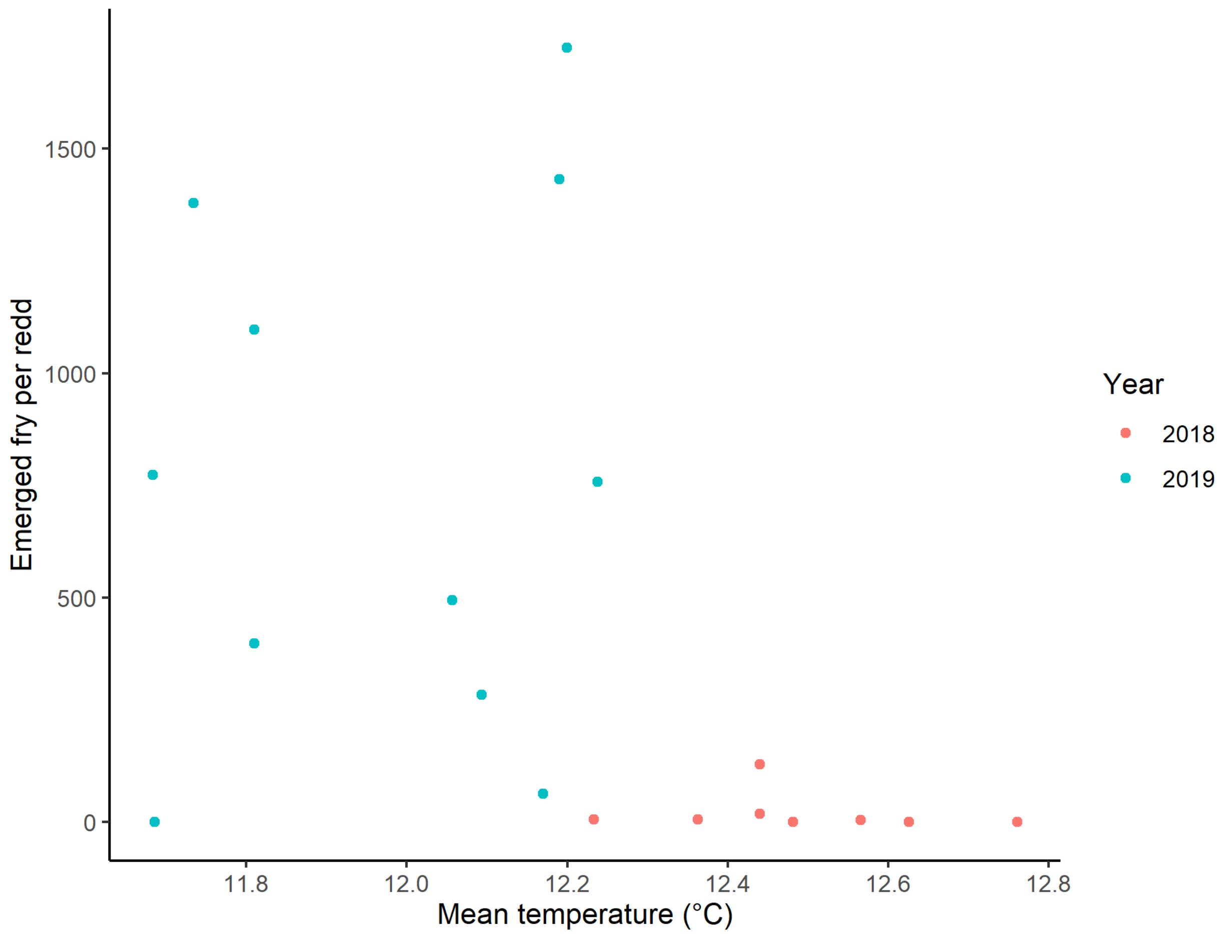

Figure 18. Total fry emergence per redd and mean temperature (°C) calculations at spring-run Chinook Salmon redds based on California Data Exchange Center (CDEC, http://cdec.water.ca.gov) gage measurements in the San Joaquin River Restoration Area in 2018 and 2019.

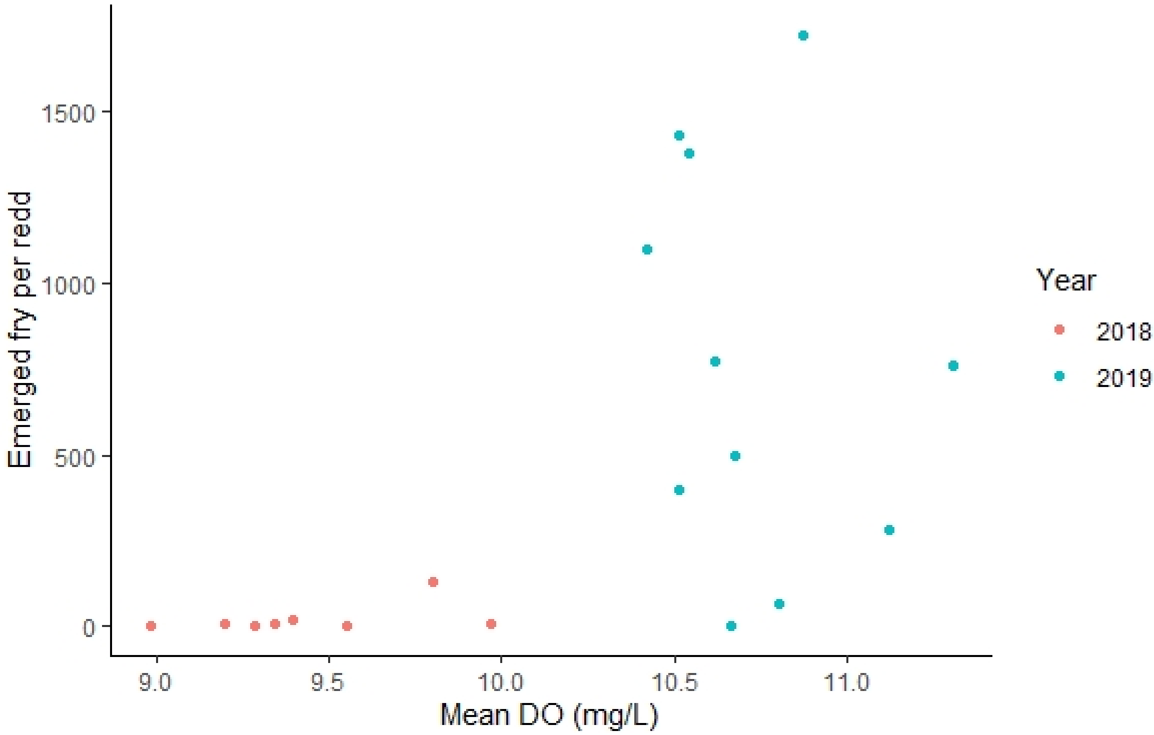

Figure 19. Total fry emergence per redd and mean dissolved oxygen (DO in mg/L) calculations at spring-run Chinook Salmon redds based on periodic field checks in the San Joaquin River Restoration Area in 2018 and 2019.

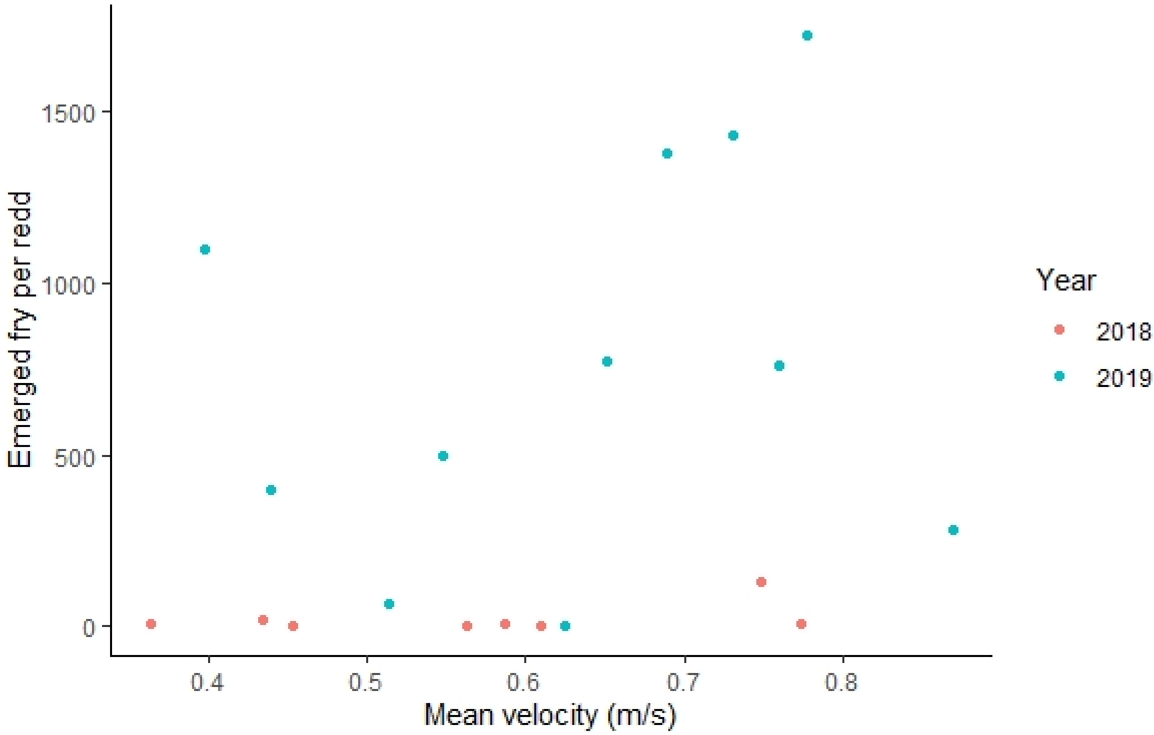

Figure 20. Total fry emergence per redd and mean velocity (m/s) calculations at spring-run Chinook Salmon redds based on periodic field checks in the San Joaquin River Restoration Area in 2018 and 2019.

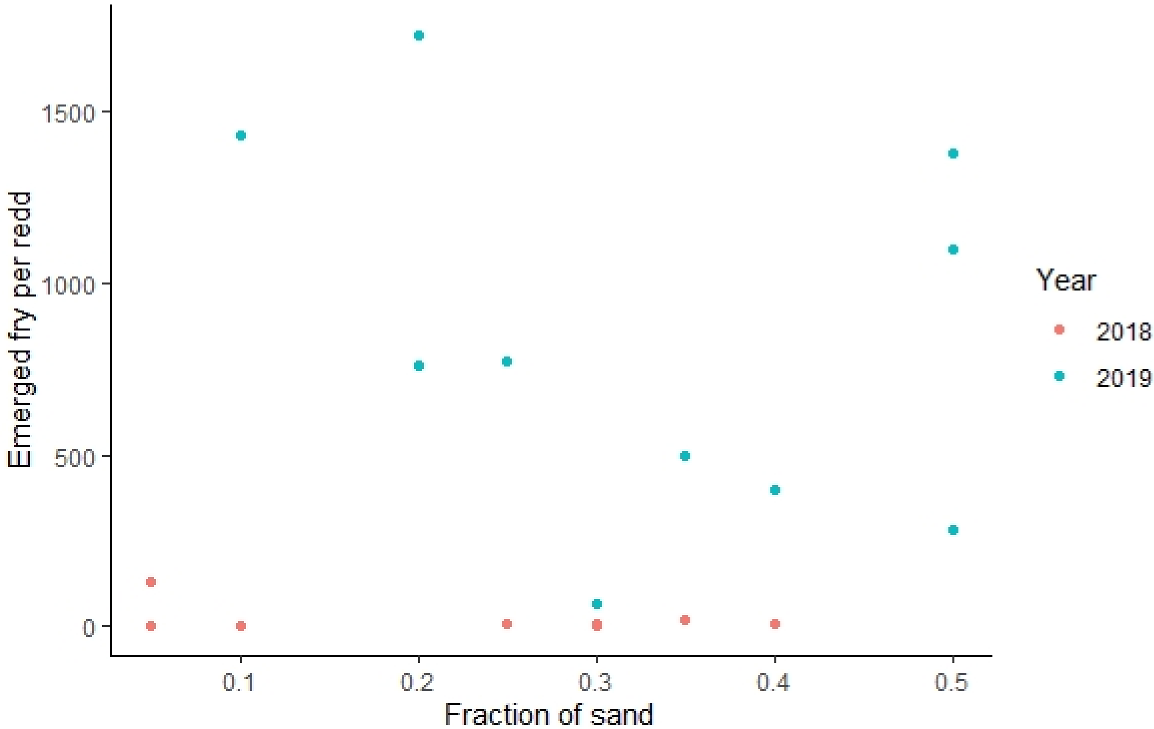

Figure 21. Total fry emergence per redd and pre-redd area fractions of sand measured during redd surveys at spring-run Chinook Salmon redds in the San Joaquin River Restoration Area in 2018 and 2019.